

画像通信

Vol. 6 No. 1 (通巻10)

目 次

第13回 画像分科会（大阪）のご案内

第14回 画像分科会（神戸）の予告

昭和58年4月

社団法人 日本放射線技術学会
画 像 分 科 会

第 13 回 画 像 分 科 会

日 時 : 昭和 58 年 4 月 1 日 (金) 6:00 pm ~ 8:00 pm

会 場 : 学会総会第 1 会場 (大阪大学松下講堂)

「画像について語ろう」

座 長 金 森 仁 志 先生 (京都工繊大)

テーマ : Scatter Suppression Technique : Current and Future
Capabilities

講 師 Gary T. Barnes 博士 (Alabama 大学教授)

このテーマは、「散乱線の抑制技術の現状とこんごの発展」という、臨地の撮影技術にとって、大変重要な課題であります。Barnes 先生は、これまでこのテーマに関しての多くの研究成完を持っておられます。今回はこのテーマを中心に講演をしていただき、そのあと自由に議論をかわしていただきます。

なお、そのために、本号は以下このテーマに関連した Barnes 先生の論文を 2, 3 転載しました参考にしていただければ幸いです。

また、「The design and performance of a scanning multiple slit assembly」は、とくに中心テーマだと考え、その大要を日本語にして、開催当日、みなさん方に配布し講演と議論のために役立てたいと思っております。

当日は、通訳の方にも手伝っていただきますので、日本語で自由に、そして活発に討論していただけるものと確信しております。

Barnes 先生の簡単な履歴と業績を掲載しております。参考にして下さい。

第 14 回 画像分科会の予告

日 時 : 昭和 58 年 10 月 29 日 (土) (予定)

場 所 : 神戸市 神戸国際会議場 (予定)

教育講演 (予定) :

「核イメージングについて」 滝 沢 正 臣 先生 (信州大学)

一般研究発表会 :

演題〆切は、昭和 58 年 9 月 10 日です。多くの演題をお寄せ下さい。簡単な抄録をついていただくと幸いです。

CURRICULUM VITAE

NAME: Gary Thomas Barnes

BUSINESS ADDRESS: Department of Diagnostic Radiology
University of Alabama School of Medicine
The University of Alabama in Birmingham
Birmingham, Alabama 35294

TELEPHONE: (205) 934-5131

BIRTHPLACE: Erie, Pennsylvania

BIRTHDATE: September 11th, 1942

CERTIFICATIONS:

Radiological Physics, American Board of Radiology, 1976

POSITIONS:

Professor, Department of Diagnostic Radiology, University of Alabama in Birmingham, 1981 - present

Associate Professor, Department of Diagnostic Radiology, University of Alabama in Birmingham, 1976 - 1981

Assistant Professor, Department of Diagnostic Radiology, University of Alabama in Birmingham, 1972 - 1976

Postdoctoral Trainee in Medical Physics, Department of Radiology and Medical Physics, University of Wisconsin, 1971 - 1972

Administrative Assistant, Office of Grants and Contracts, Wayne State University, Summer, 1971

Research Assistant, Department of Physics, Wayne State University, 1965 - 1971

Teaching Assistant, Department of Physics, Wayne State University, 1965

PROFESSIONAL AND SCIENTIFIC SOCIETIES:

American Association of Physicists in Medicine
President, Southeastern Chapter 1979 - 1980

American College of Radiology

American Physical Society

Health Physics Society
President, Alabama Chapter 1981 - 1982

Radiological Society of North America

NATIONAL COMMITTEE APPOINTMENTS:

American Association of Physicists in Medicine
Training of Radiologist Committee, 1977 - 1979
Finance Committee, 1978 - 1980
Diagnostic Radiology Committee, 1980 - ; Chairman, 1981 -
Science Council, 1981 -
Board of Directors, 1981 -
Associate Editor, MEDICAL PHYSICS, 1982 -

American Board of Radiology
Guest Examiner - Oral Boards, 1981 -

American College of Radiology
Learning Laboratory Physics Accession Committee, 1979 -
Equipment Commission Committee on Purchase and Acceptance
Specifications, 1981
Physics Commission Committee on Education, 1982

Radiological Society of North America
Editorial Advisory Board, RADIOLOGY, 1980 -
Scientific Program Committee, 1980 - 1982
Associated Sciences Committee, 1982 -

ACTIVITIES RELATED TO UAB

Radiation Safety Committee, 1976 -

Radioactive Drug Research Committee, 1976 -

PUBLICATIONS

1. Gustafson DR, Barnes GT: Effect of Magnetic Field Orientation on Positron Annihilation in Potassium. *Phys Rev Letters* 18:3-5, 1967.
2. Barnes GT, Gustafson DR: Positron Annihilation in Plutonium, pp 271 - 278 in *Plutonium 1970 and Other Actinides*, edited by W.N. Miner, The Metallurgical Society AIME, Inc., New York, 1970.
3. Gustafson DR, Barnes GT: Investigation of Self-Irradiation Damage in Plutonium. *J Nucl Materials* 48:79-85, 1973.
4. Barnes GT, Witten DM: Film/Screen Considerations in Tomography. *Radiology* 113:477-479, 1974.
5. Barnes GT, Cleare HM, Brezovich IA: Improvement of Contrast and/or Reduction of Patient Exposure in Diagnostic Radiology by Means of a Scanning Multiple Slit Assembly, pp 791-796 in *Operational Health Physics, Proceedings of the Ninth Midyear Topical Symposium of the Health Physics Society held in Denver, CO, February 9-12, 1976*, edited by P.L. Carson, W.R. Hendee and D.C. Hunt.
6. Barnes GT, Cleare HM, Brezovich IA: Reduction of Scatter in Diagnostic Radiology by Means of a Scanning Multiple Slit Assembly. *Radiology* 120:691-694, 1976.
7. Barnes GT: The Dependence of Radiographic Mottle on Beam Quality. *Am J Roentgenol* 127:819-824, 1976.
8. Barnes GT, Nelson RE, Witten DM: A Comprehensive Quality Assurance Program--a Report of Four Year's Experience at The University of Alabama in Birmingham. *Optical Instrumentation in Medicine V, Proc. of the SPIE* 96:19-25, 1976.
9. Barnes GT, Brezovich IA, Witten DM: The Scanning Multiple Slit Assembly: A Practical and Efficient Device to Reduce Scatter. *Am J Roentgenol* 129:497-501, 1977.
10. Nelson RE, Barnes GT, Witten DM: An Economic Analysis of a Quality Assurance Program. *Radiol Technol* 49:129-134, 1977.
11. Brezovich IA, Barnes GT: A New Kind of Grid. *Med Phys* 4:451-453, 1977.
12. Barnes GT, Brezovich IA: Contrast - The Effect of Scatter, pp 73 - 81 in *Breast Carcinoma - The Radiologist's Expanded Role*, edited by W.W. Logan, John Wiley & Sons, Inc., New York, 1977.
13. Brezovich IA, Barnes GT: The Effect of Electron Evaporation on X-Ray Tube Current. *Optical Instrumentation in Medicine VI, Proc. of the SPIE* 127:175-179, 1977.
14. Yester MV, Barnes GT: Geometrical Limitations of Computed Tomography (CT) Scanner Resolution. *Optical Instrumentation in Medicine VI, Proc. of the SPIE* 127:296-303, 1977.
15. Barnes GT, Brezovich IA: The Intensity of Scattered Radiation in Mammography. *Radiology* 126:243-247, 1978.
16. Barnes GT, Yester MV, King MA: Optimizing Computed Tomography (CT) Scanner Geometry. *Optical Instrumentation in Medicine VII, Proc. of the SPIE* 173:225-237, 1979.

17. Barnes GT, Brezovich IA: The Design and Performance of a Scanning Multiple Slit Assembly. *Med Phys* 6:197-204, 1979.
18. Barnes GT: Characteristics of Scatter, pp 223-242 in Reduced Dose Mammography, edited by W.W. Logan and E.P. Muntz, Masson Publishing USA, Inc., New York, 1979.
19. King MA, Barnes GT, Yester MV: A Mammographic Scanning Multiple Slit Assembly: Design Considerations and Preliminary Results, pp 243-252 in Reduced Dose Mammography, edited by W.W. Logan and E.P. Muntz, Masson Publishing USA, Inc., New York, 1979.
20. Barnes GT: The Use of Bar Pattern Test Objects in Accessing the Resolution of Film/Screen Systems, pp 138-151 in The Physics of Imaging: Recording System Measurements and Techniques, edited by A.K. Haus, American Institute of Physics, New York, 1979.
21. Barnes GT: Imaging System Considerations in Conventional Thin Section Tomography, pp 483-491 in The Physics of Imaging: Recording System Measurements and Techniques, edited by A.K. Haus, American Institute of Physics, New York, 1979.
22. Wagner RF, Barnes GT, Askins BS: Effect of Reduced Scatter on Radiographic Information Content and Patient Exposure: A Quantitative Demonstration. *Med Phys* 7:13-18, 1980.
23. Brezovich IA, Barnes GT: An Investigation and Explanation of the Fall-Off of X-Ray Tube Current During an Exposure. *Phys Med Biol* 25:241-249, 1980.
24. Barnes GT, Moreland RF, Yester MV, Witten DM: The Scanning Grid: A Novel and Effective Bucky Movement. *Radiology* 135:765-767, 1980.
25. Barnes GT: Principles of Slit Radiography, pp 123-132 in Optimization of Chest Radiography, Proceedings of a Symposium held in Madison, WI, April 30 - May 2, 1979, edited by J.R. Cameron, A.J. Alter and J.F. Wochos, U.S. Department of Health and Human Services Publication: (FDA) 80-8124, 1980.
26. Wagner LK, Haus AG, Barnes GT, Bencomo JA, Amtey SR: Comparison of Methods Used to Measure the Characteristic Curve of Radiographic Screen/Film Systems. *Optical Instrumentation in Medicine VII*, Proc. of the SPIE, 233:7-10, 1980.
27. Barnes GT, McDanal W: When is Inhouse Service Cost Effective? *Optical Instrumentation in Medicine VIII*, Proc. of the SPIE 233:286-290, 1980.
28. Yester MV, Barnes GT, King MA: Kilovoltage Bootstrap Sensitometry. *Radiology* 136:785-786, 1980.
29. Barnes GT, Moreland RF, Yester MV: Exposure Reduction in Medical Radiography Utilizing a Scanning Grid, pp 307-313, in Medical Health Physics, Proceedings of the Fourteenth Midyear Topical Symposium of the Health Physics Society held in Hyannis, MA, December 8-12, 1980, edited by T.G. Martin and K.W. Price.
30. Yester MV, Barnes GT, King MA: Experimental Measurements of the Scatter Reduction Obtained in Mammography with a Scanning Multiple Slit Assembly. *Med Phys* 8:155-162, 1981.
31. Barnes GT, Moreland RF: A Linear Tomographic Alignment Test Object. *Radiology* 141:247-249, 1981.

32. Mattson RA, Sones RA, Stickney JB, Tesic MM, Barnes GT: The Design and Physical Characteristics of a Digital Chest Unit. *Digital Radiography, Proc. of the SPIE*, 314:160-163, 1981.
33. Barnes GT, Witten DM: Image Quality - An Educational and Scientific Problem. *Radiology* 143:277, 1982.
34. Barnes GT: Radiographic Mottle - A Comprehensive Theory. *Med Phys* 9:656-667, 1982.
35. Barnes GT, Chakraborty DP: Radiographic Mottle and Patient Exposure in Mammography. *Radiology* 145:815-821, 1982.

PUBLICATIONS IN PRESS

1. King MA, Barnes GT: Exposure Uniformity Considerations in Slit Radiography. *Med Phys*.
2. Chakraborty DP, Barnes GT: Signal-to-Noise Ratio Considerations in Radiographic Imaging. *Med Phys*.
3. Wagner LK, Barnes GT, Bencomo JA, Haus AG: An Examination of Errors in Characteristic Curve Measurements of Radiographic Screen/Film Systems. *Med Phys*.

PAPERS SUBMITTED FOR PUBLICATION

1. Tesic MM, Mattson RA, Barnes GT, Sones RA, Stickney MS: A Prototype Digital Chest Unit - Design Features and Considerations. *Radiology*.
2. Fraser RG, Breatnach E, Barnes GT: Digital Radiography of the Chest - Clinical Experience with a Prototype Model. *Radiology*.

BOOKS AND CHAPTERS

1. Dubovsky EV, Barnes GT, Beschi RJ, Logic JR, Russell CD, Sims JC and Tubin M: Nuclear Medicine Technology Continuing Education Review, Medical Examination Publishing Co., Inc., Flushing, New York, 1976.
2. Barnes GT, Tishler JM: Fluoroscopic Image Quality and Its Implications Regarding Equipment Selection and Use. Chapter 8, pp 93-106, in The Physical Basis of Medical Imaging, edited by C.M. Coulam, J.J. Erickson, A.E. James and F.D. Rollo, Appleton-Century-Crofts, New York, 1981.
3. Barnes GT: Basic Atomic and Nuclear Physics. Chapter 1, pp 1-9; Radioactive Decay. Chapter 2, pp 10-19; Detectors and Instrumentation. Chapter 3, pp 20-29; Imaging. Chapter 4, pp 30-44; Dosimetry. Chapter 5, pp 45-57; in Nuclear Medicine Technology Continuing Education Review, edited by E.V. Dubovsky, Medical Examination Publishing Co., Inc., Garden City, New York, 1981 (Second Edition).
4. Barnes GT: Contributing Editor, Medical Physics Data Book - (NBS Handbook 138) edited by T.W. Padikal and S.P. Fivozinsky. U.S. Government Printing Office, Washington, D.C. Issued March, 1982.

PATENTS

1. Barnes GT: Method and Apparatus for Reduction of Scatter in Diagnostic Radiology. U.S. Patent No. 4,096,391. Issued June 20th, 1978.
2. Barnes GT: Multiple Beam Computed Tomography (CT) Scanner. U.S. Patent No. 4,315,157. Issued February 9th, 1982.
3. Barnes GT: Scanning Grid Apparatus for Suppressing Scatter in Radiographic Imaging. U.S. Patent No. 4,340,818. Issued June 20th, 1982.

The design and performance of a scanning multiple slit assembly

Gary T. Barnes and Ivan A. Brezovich^{a)}

Department of Diagnostic Radiology, University of Alabama School of Medicine, The University of Alabama in Birmingham, Birmingham, Alabama 35233

(Received 14 April 1978; accepted for publication 24 October 1978)

A scanning multiple slit assembly (SMSA) has been constructed for the purpose of reducing scatter in medical radiography. The SMSA consists of a series of long, narrow beam-defining slits above the patient that are aligned and synchronously moved with scatter-eliminating slots beneath the patient during an exposure. Evidence, based on measurements of the ratio of scattered-to-primary radiation imaged and radiographs of patients, is presented indicating that such a device is a practical and efficient method of reducing scatter and improving contrast compared to conventional grids. The design considerations and trade-offs associated with the choice of slit width, slit separation distance, and aft slot depth are discussed along with the effect of these parameters on the SMSA's performance. The various problems encountered in obtaining a uniform scan and the manner in which they were handled are also discussed.

I. INTRODUCTION

Scattered x-ray photons, when imaged, degrade the radiographic image by reducing contrast. The fraction of primary beam or possible contrast that is imaged due to the presence of scatter or the scatter degradation factor (SDF) can be expressed as:¹

$$\text{SDF} = (1 + s/p)^{-1}, \quad (1)$$

where s/p is the ratio of scattered-to-primary radiation. The contrast-reducing effect of scattered x rays is a well known phenomenon, but it is not usually appreciated that a relatively small amount of scatter will result in a significant loss of contrast. This fact is illustrated in Fig. 1 which is the plot of the SDF versus s/p . Investigations have shown that there is a practical upper limit of ~94% in the efficiency with which a grid can remove scatter.²⁻⁴ In cases in which the relative intensity of scatter is not large (~1-2) as in the lung field in chest radiography,^{5,6} high ratio grids are capable of obtaining 90% of the primary beam or possible contrast. However, where the ratio of scattered-to-primary is large (~8) as in the abdomen,⁶ even with the highest ratio grids, only 50% to 60% of the primary beam contrast is imaged and significant improvement in contrast will result with a superior method of scatter reduction.

Figure 2 shows a scanning multiple slit assembly (SMSA) constructed at the University of Alabama in Birmingham (UAB) which has a higher scatter elimination efficiency and a higher primary transmission than conventional grids. A description of the device and some preliminary results have been presented elsewhere⁷ and this paper describes the design considerations and compares the performance of the unit, both quantitatively and qualitatively to conventional Bucky grids. The principle of the SMSA is illustrated in Fig. 3. An array of beam defining fore slits are positioned above the patient. The fore slits⁸ are aligned and synchronously moved with scatter-eliminating slots⁸ beneath the patient during an

exposure. The small field size of the long, narrow beams of radiation defined by the former results in a small amount of scatter being associated with a given beam, while very little scatter contribution arises from neighboring beams due to their separation and the grid ratio of the aft slots. Another important feature of the SMSA is that very few of the information carrying primary x rays emerging from the patient are attenuated by the aft slots.

The use of a set of moving slits fore and aft of the patient to reduce scattered radiation was suggested as early as 1903⁹ and several references to the technique have subsequently appeared in the literature.¹⁰⁻¹² However, due to the long exposure time required and the successful development of the Bucky diaphragm,^{13,14} this method of scatter reduction has not come into common use. Only when a device employing a multiplicity of slits was suggested,¹⁵⁻²⁰ along with the availability of high capacity x-ray tubes and fast intensifying screens, did scatter reduction techniques using fore and aft slits appear to be feasible.

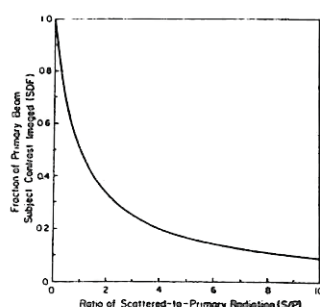
II. DESIGN CONSIDERATIONS

A. General requirements

The general requirements that were deemed essential in order for the SMSA to be useful for abdominal radiography are (1) reasonable patient access and comfort, (2) a uniform scan of the patient, and (3) an exposure time of $\frac{1}{2}$ s or less. The desire to obtain roughly the same magnification as a conventional unit and the fact that the aft slots require more space than a grid dictated that a 121.9 cm SID be employed with the table top located ~8 cm above the image plane. Considerations of patient access and comfort limited the distance between the focal spot and the fore slits to ~50 cm and resulted in a patient clearance (~60 cm) comparable to a conventional 101.6 cm SID system.

Since the patient is scanned by a small number of long,

FIG. 1. Plot of the fraction of primary beam contrast imaged or SDF vs s/p .



narrow beams of radiation in a short period of time, it is desirable, in order to obtain a uniform exposure, that the radiation output be essentially constant rather than pulsating. This requirement was satisfied by employing a three-phase (3ϕ) generator having 12 rectifying elements. Such generators are in common use and have an almost constant tube voltage ($\sim 3.4\%$ ripple) when energized. Another consideration in obtaining a uniform exposure requires that the x-ray production terminate precisely when the SMSA has moved through an integral number of slit intervals. If this condition is not satisfied, then a certain amount of start/stop radiation overlap will occur resulting in a grid line type of effect. The easiest way that this requirement can be satisfied is for the production of x rays to be initiated and terminated by the SMSA. This was accomplished by employing a generator with forced commutation or extinction. Also, the greater the number of slit intervals that the assembly scans through during an exposure the less apparent any start/stop radiation overlap will be. The SMSA scan distance was limited by space and acceleration requirements to 8 slit intervals.

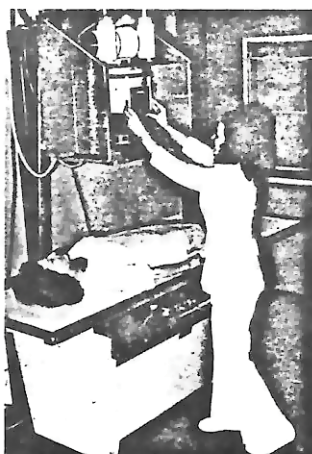


FIG. 2. SMSA constructed in simulated clinical use. A 121.9 cm SID is employed with the fore slits located 48.8 cm below the focal spot. The fore slit width and spacing between slits are 1.63 and 6.50 mm, respectively (i.e., 1.23 slits/cm). The aft slots are located between the tabletop and the plane of the image receptor with the bottom of the aft slots 1.9 cm above the latter. They are 3 cm deep, 4 mm wide and separated by 16 mm of lead (i.e., 0.5 slots/cm). Thirty-nine fore slits and aft slots are employed and during an exposure any region of the patient is sequentially scanned by eight different beams of radiation.

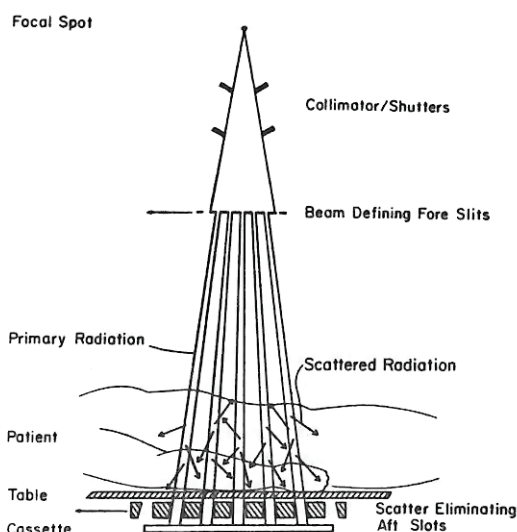


FIG. 3. Principle of SMSA.

A substantial increase in tube loading results with the SMSA (~ 7 times) compared to conventional systems because of its greater SID and because 80% of the beam defined by the collimator is attenuated by the fore slits prior to being incident on the patient. This is a limiting constraint since it is desirable to have an exposure time of $1/2$ s or less so that peristolic and other types of involuntary patient motion do not noticeably degrade image quality. Three-phase radiographic techniques routinely employed at UAB for different patient thicknesses are listed in Table I along with the anticipated mAs required for the SMSA. Assuming a $1/3$ -s exposure time, the power requirements for the SMSA techniques of Table I are tabulated in Table II. Table III gives $1/3$ -s kW ratings for a 12° , 100-mm-diam target x-ray tube for different size focal spots. The kW rating of the 1.2-mm focal spot allows for SMSA exposure times of $1/3$ s or less for patients of greater than 30 cm thickness. Shorter exposure times are possible if a faster image receptor than Kodak RPL film combined with DuPont Hi Plus screens is employed.

B. Selection of slit width, slit spacing, and slot depth

Scatter/primary ratios and the distribution of scatter in the plane of the image receptor were measured as a function

TABLE I. Comparison of 3ϕ 12:1 grid and SMSA techniques.^a

Patient thickness (cm)	X-ray tube voltage (kVp)	X-ray tube current \times time (mAs) 12:1 grid ^b	SMSA ^c
20	76	30	216
25	96	30	216
30	112	30	216

^a For Kodak RPL film combined with DuPont Hi Plus screens.

^b 101.6 cm SID.

^c 121.9 cm SID and 20% field coverage by fore slits.

TABLE II. X-ray tube power requirements for SMSA techniques.^a

Patient thickness (cm)	Required power (kW)
20	49
25	62
30	73

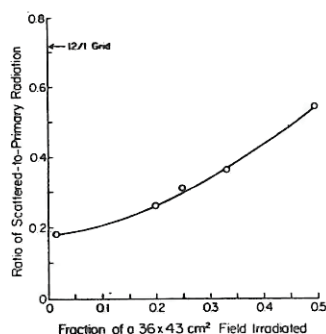
^a For 1/3 s exposure time.

of slit width and slot depth for a single long, narrow beam geometry and can be used to calculate the anticipated performance of the SMSA for certain design configurations. The results of these measurements along with the calculation of the s/p transmitted for a given SMSA slit width, slot depth and separation distance have been presented elsewhere.^{17,18} In Fig. 4 the calculated s/p ratio transmitted by a SMSA having 0.5-cm-wide and 3.0-cm-deep aft slots is plotted for different separation distances or fractional coverage by the beam defining fore slits of the area of interest. In Figs. 5 and 6 the effect on the transmitted s/p ratio of varying the aft slot depth and the fore slit and aft slot width respectively is illustrated for 20% coverage by the fore slits of the area of interest. The calculated values in Figs. 4-6 are for a 20-cm-thick, 36×43 cm Lucite phantom irradiated by an 80 kVp (1 ϕ) x-ray beam and have been corrected for the loss of primary due to the unsharpness of the fore slits at the aft slots. The previously reported data was measured with a 0.6 mm focal spot and a fore slit magnification at the aft slot of 1.5; whereas, for the SMSA the respective values are 1.4 mm and 2.46. In Figs. 4-6 the s/p transmitted by a 12:1, 31.5 lines/cm grid measured under similar conditions is noted for comparison.

A significant gain in scatter reduction is evidenced in Fig. 4 when the field of coverage is reduced from 50% to 20%. However, decreasing the field of coverage further does not result in appreciable reduction in scatter, but would require an exposure time of greater than $1/2$ s. Figure 5 indicates that scatter can be reduced for a given aft slot width and field of coverage by utilizing deeper aft slots. In practice, aft slot depth is limited by the desired radiographic magnification, which, for comparison purposes, was made the same as a conventional Bucky system for an object 10 cm above the tabletop. This dictated that a 7.6 cm distance between the tabletop and image plane be employed, which, allowing for clearances, limited the aft slot depth to 3.0 cm. Since greater radiographic magnifications are often acceptable and occasionally desired by radiologists, gains in scatter reduction are

TABLE III. The $1/3$ -s kilowatt ratings for different-sized x-ray-tube focal spots.^a

Nominal focal spot size (mm)	X-ray tube rating (kW)
0.6	32
1.0	58
1.2	82
2.0	115

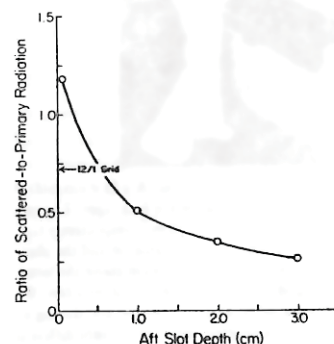
^a Sapphire 12° target x-ray tube utilizing high speed anode rotation (Ref. 21).FIG. 4. Plot of imaged s/p vs fraction of a 36×43 cm field irradiated for SMSA with 5 mm wide and 3 cm deep aft slots illustrating the effect of varying the separation distance between slits.

possible by increasing the aft slot depth in future SMSA designs.

Figure 6 indicates that major gains in the performance of the SMSA can be realized by decreasing the aft slot width for a given aft slot depth and radiation field of coverage. However, this gain is eventually limited by the loss of primary radiation due to the geometrical unsharpness of the fore slits at the level of the aft slots. This phenomenon is conceptually illustrated in Fig. 7(a). In Fig. 7(b), the primary transmission by the aft slot of the radiation beam defined by the fore slits is plotted for the SMSA geometry and a 1.4 effective focal spot size (i.e., a typical value measured for a 1.2 mm nominal focal spot size). Figure 7(b) indicates that a significant loss of primary radiation occurs for aft slot widths much less than 5 mm. It should be noted also that for aft slot widths less than 2.5 mm only a portion of the focal spot is subtended resulting in an even greater tube loading problem. Consideration of these factors resulted in the aft slot width and spacing being 4 and 16 mm, respectively (i.e., 20% coverage of the area of interest).

C. Fore slit and aft slot alignment

Because of the depth of the aft slots and their high grid ratio (7.5:1), they actually consist of two sets of lead plates 3 cm apart. The plates are composed of slits whose size and spacing are determined by the projection of the fore slits onto each of the respective planes. The fore slits and each set of the aft plates are connected by a linkage arm which pivots about the focal spot of the x-ray tube. This eliminates any grid cutoff by the aft slots and maintains alignment of three plates during the scan.

FIG. 5. Plot of imaged s/p vs aft slot depth for SMSA with 5-mm-wide aft slots and 20% coverage of a 36×43 cm field.

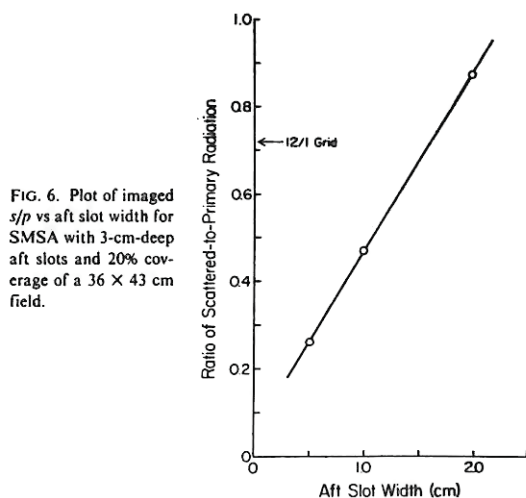


FIG. 6. Plot of imaged s/p vs aft slot width for SMSA with 3-cm-deep aft slots and 20% coverage of a 36×43 cm field.

D. Motor-generator interface

A dc servomotor and controller are used to drive the SMSA and the generator was rewired so that the scanning motion controls the exposure start and stop signals. When the x-ray exposure button is pushed, after a preset delay which allows the x-ray tube rotor to reach its operating speed, the scanning motion is initiated. When the aft slot assembly has moved through a distance of ~ 7 cm and reached a uniform velocity, a position sensor turns on the generator. The exposure is terminated by a second position sensor after the unit has scanned a distance of 16 cm (i.e., 8 slit intervals in the plane of the lower aft slot plate).

E. Scan uniformity problems

Even though the effect of start/stop radiation overlap was minimized by employing a three phase generator equipped with forced extinction and by sequentially scanning a given area of the film by 8 or more slits, several design problems were realized during the initial testing phase which contributed to a nonuniform film exposure. These were (1) vibrational problems, (2) motor velocity overshoot at the time of the initiation of the exposure, and (3) mA falloff during the exposure. The first of these problems was eliminated by increasing the rigidity of the tube stand. The second problem was associated with the method of velocity regulation employed by the DC servomotor and controller. A tachometer attached to the drive shaft of the electric motor generates a DC voltage proportional to the speed of the motor. This tachometer voltage is fed to the motor control unit which compares it to the voltage of a preselected velocity command signal. The output of the control unit drives the motor in a direction and at a speed so that the difference between the tachometer and command signal vanishes. However, motor overshoot problems occurred because of a delay between the generation of the signal and response of the control. Internal adjustments were made in the motor controller which reduced this delay as much as possible. Also, more time was

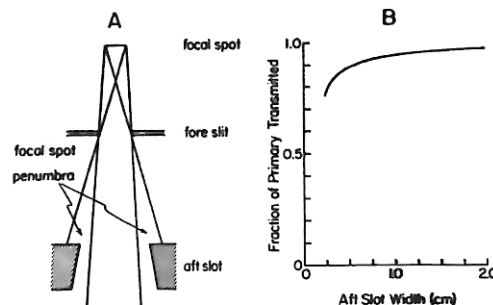


FIG. 7. Loss of primary due to unsharpness of fore slits at aft slots. (a) Geometry of focal spot, fore slit, and aft slot. (b) Plot of primary transmission vs aft slot width for 1.4 mm effective focal spot and 2.46 magnification of fore slit at aft slot.

allowed for the motor to reach its operating speed before initiating the start of the x-ray exposure.

After the two problems discussed above were minimized, uniform scans were still not achieved. Further investigation resulted in the observation that the radiation intensity from the x-ray tube decreased exponentially with time and reached an equilibrium value ~ 400 ms after the start of the exposure. Upon examination of various factors affecting the radiation output, this falloff was attributed to a corresponding falloff in x-ray tube current. An example of this phenomenon is illustrated in Fig. 8(a). Upon further investigation, this effect was observed on x-ray generators and on tubes of several different manufacturers. The x-ray generators that exhibit this phenomenon all employ "open circuit" mA stabilization utilizing a constant voltage transformer. A few manufacturers employ "closed circuit" mA stabilization (i.e., feedback circuit) and their units exhibit a constant tube current with time except for ripple associated with the AC filament heating power. The magnitude of the observed falloff was a function of mA, kV, x-ray tube filament and the type of generator (i.e., single-phase or three-phase). Typically, it is on the order of 15% for three-phase generators and 6% for single-phase generators.

The phenomenon was attributed to the cooling effect due to the thermionic emission or evaporation of electrons from the filament, and a comprehensive theory describing the qualitative and quantitative features of the phenomenon is described elsewhere.²² To correct for this effect, a simple mA stabilization circuit was built. It consists basically of a resistor

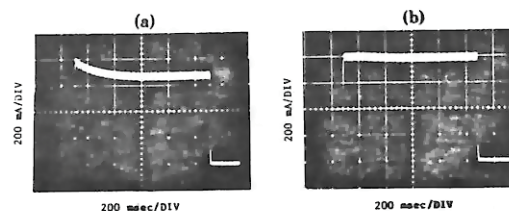


FIG. 8. Oscilloscope traces of x-ray tube current vs time for large focal spot of GE Maxiray 75, 1.0/2.0 mm focus, Model No. 11DB6A1 x-ray tube at 800 mA and 60 kVp (3 ϕ): (a) without correcting for cooling effect of electrons evaporating from the filament; (b) correcting for cooling effect.

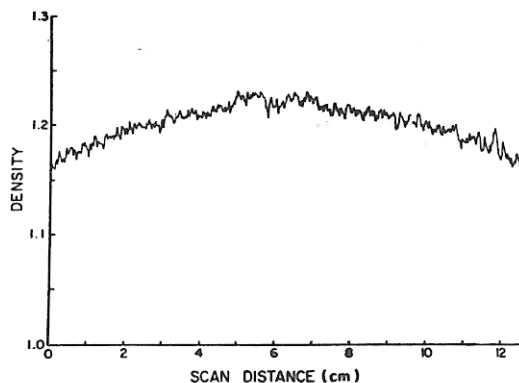


FIG. 9. Microdensitometer trace of SMSA radiograph (Kodak RPL film/DuPont Hi Plus screens) of Lucite phantom illustrating scan uniformity achieved. Technique factors were 90 kVp, 600 mA and $\frac{1}{2}$ s. The trace was obtained with a Joyce-Loebl microdensitometer having a 0.2×4 mm aperture with the former dimension aligned with direction of SMSA and microdensitometer scanning movement.

in series with the primary of the filament transformer. During the exposure the resistor is short circuited by a relay boosting the filament power by an amount sufficient to compensate for the power carried away by the evaporating electrons. By a proper choice of the resistor, the tube current could be made constant throughout the exposure as illustrated in Fig. 8(b).

The scan uniformity finally achieved with the unit is illustrated in Fig. 9. No noticeable periodic density nonuniformity is apparent at 2.0 cm intervals (i.e., SMSA's slit interval) or for that matter at any other interval in the microdensitometer trace of Fig. 9. A slight but clinically unimportant 2.0 cm periodic density variation is apparent upon close visual inspection of the radiograph scanned for Fig. 9 and similar radiographs. Furthermore, once the SMSA was aligned, no difficulty was experienced or subsequent adjustment required in producing such radiographs over a period of several months.

III. PERFORMANCE OF SMSA

A. Quantitative

The quantitative evaluation of the SMSA's performance involved measurements which compared the relative intensity

TABLE IV. Ratio of scattered-to-primary radiation transmitted by SMSA and commonly used grids for different x-ray tube voltages.^a

Scatter reduction technique	60 kVp	80 kVp	100 kVp	120 kVp
None	5.5	6.6	7.2	7.1
8:1 grid ^(b)	0.72	1.0	1.2	1.4
12:1 grid ^(b)	0.48	0.62	0.76	0.87
SMSA	0.16	0.20	0.22	0.22

^a Determined employing an 18-cm-thick, 30 X 30 cm Lucite phantom.

^b Fibre interspace grids having 31.5 lines/cm and respective lead contents of 363 and 572 mg/cm².

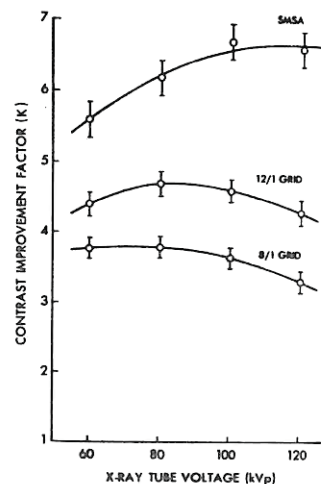


FIG. 10. Plot of contrast improvement factor (K) of commonly used grids, and SMSA vs kVp.

of scatter imaged with the SMSA to that of commonly used grids under similar conditions. The measurement technique employed consisted of placing a small lead beam stop centrally on a phantom. The x rays imaged beneath the beam stop are due to scatter; whereas beneath the rest of the phantom they are due to scatter plus primary. The scattering phantom employed was an 18-cm-thick, 30 X 30 cm block of Lucite. A film-screen combination was employed as an image receptor and sensitometry was used to convert the densities obtained to relative exposure values. To reduce the effect of random errors, six runs were made and the results averaged. To correct for the systematic experimental error associated with the perturbation of the scatter radiation field by the beam stop, each run employed a series of stops ranging in diameter from 7 to 12 mm, which allowed for a linear regression interpolation to a zero area beam stop. This is a significant correction when scatter reduction techniques are employed due to the increased percentage of small angle scatter.

The relative intensity of scatter transmitted by an 8:1 grid, a 12:1 grid and the SMSA was measured at 60, 80, 100, and 120 kVp. These results along with the relative intensity of scatter when no scatter reduction technique is employed are tabulated in Table IV. The observed standard deviations of the six runs made for each s/p ratio was typically 6% of the tabulated values. The significance of the beam stop correction was typically 8%, 11%, and 15% for the 8:1 grid, 12:1 grid, and SMSA, respectively. The correction was negligible without a scatter reduction technique. The results are in reasonable agreement with published grid data^{2,4,6,18} and with that projected for the SMSA at 80 kVp (0.23) from the calculations plotted in Fig. 6 for a slightly larger phantom. The amount of scatter imaged with the SMSA was considerably less than that of both the 12:1 grid ($\sim 1/3$) and that of the 8:1 grid ($\sim 1/5$).

The contrast improvement factor (K) of a scatter reduction technique is a ratio of the SDF with the technique to that without and can be calculated using Eq. (1) from the data in Table IV. The K 's so calculated are plotted in Fig. 10. De-

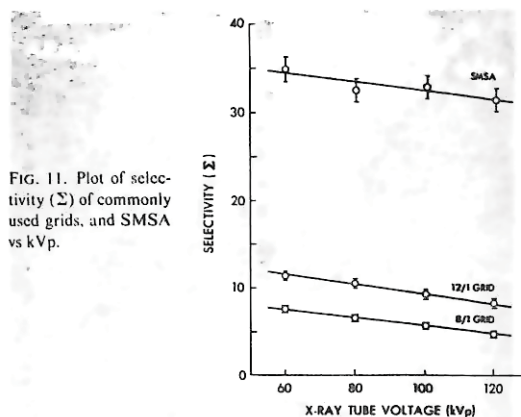


FIG. 11. Plot of selectivity (Σ) of commonly used grids, and SMA vs kVp.

is relatively independent of the scattering geometry is its selectivity, Σ , which is defined as the ratio of primary transmission-to-scatter transmission of the grid. This can also be calculated in a straightforward manner from the data in Table IV and is compared as a function of kVp in Fig. 11 for the SMA and grids studied. The noticeably larger selectivity of the SMA is due to its greater primary transmission in addition to its smaller scatter transmission. The falloff in the selectivity of conventional grids with increasing kVp's is due to the increased scatter penetration of the lead strips comprising the grid. It is interesting to note that the selectivity of the SMA has little beam quality dependence from 60 to 120 kVp (i.e., a 9% decrease compared to 35% and 28% for the 8:1 and 12:1 grids).

B. Qualitative

In order to determine the clinical performance of the SMA, a qualitative evaluation was performed which consisted of a series of patient comparison films between the SMA and commonly used grids. The diagnostic implications of the comparison films will be presented elsewhere.²⁴ Figure 12 compares lateral sacral spine radiographs obtained at the same kVp with the SMA and a 12:1 grid. The improvement in radiographic contrast obtained with SMA was

pending on kVp, the contrast improvement of the SMA is ~50%-100% greater than that of the 8:1 grid and ~25%-50% greater than that of the 12:1 grid for the scattering situation measured.

The contrast improvement factor of a scatter reduction technique depends on the amount of scatter emerging from a patient or phantom. A parameter of grid performance that

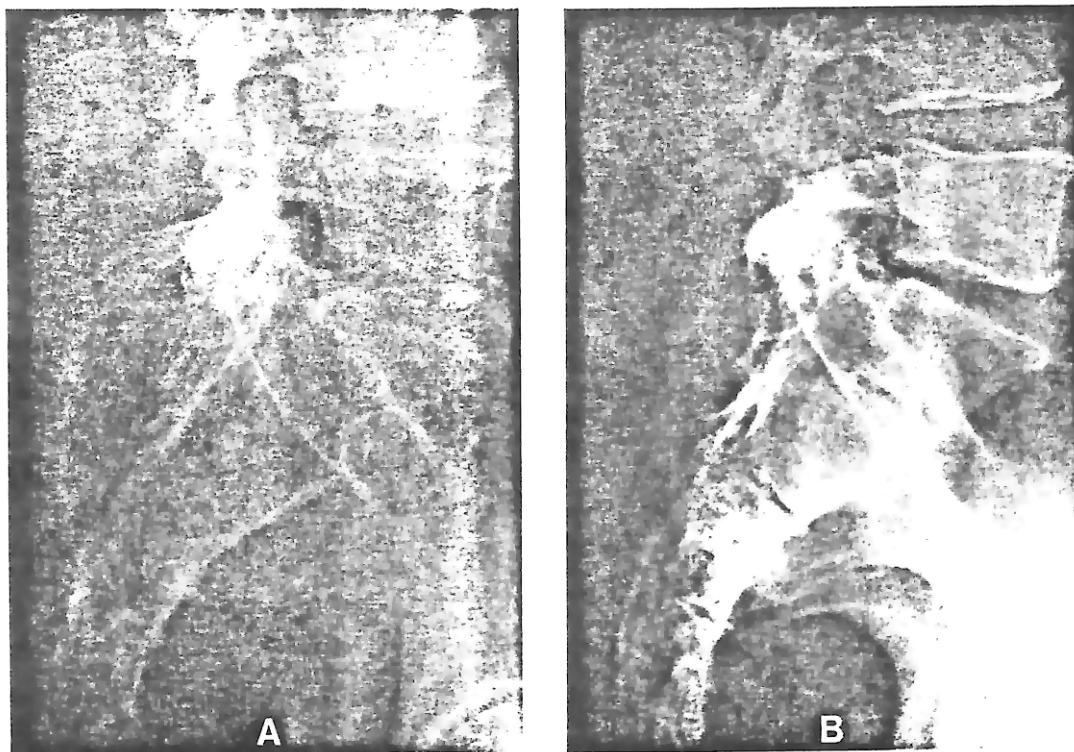


FIG. 12. Comparison lateral sacral spine radiographs at 116 kVp (3 Φ). Subject measured 33 cm and radiation field was 20 cm \times 30 cm: (a) 12:1, 40.6 lines/cm grid using 300 mA at 0.07 s, 102 cm SID, 520 mR entrance skin exposure; (b) SMA using 600 mA at 1/3 s, 122 cm SID, 760 mR entrance skin exposure. Both exposures employing a nominal 1.2 mm focal spot with same cassette using Kodak Lanex screens combined with Kodak Ortho-G film. The films were developed within minutes of each other in the same processor. The same generator was employed for both films and the HVL's of the two source assemblies used were matched at 3.9 mm of Al at 80 kVp.

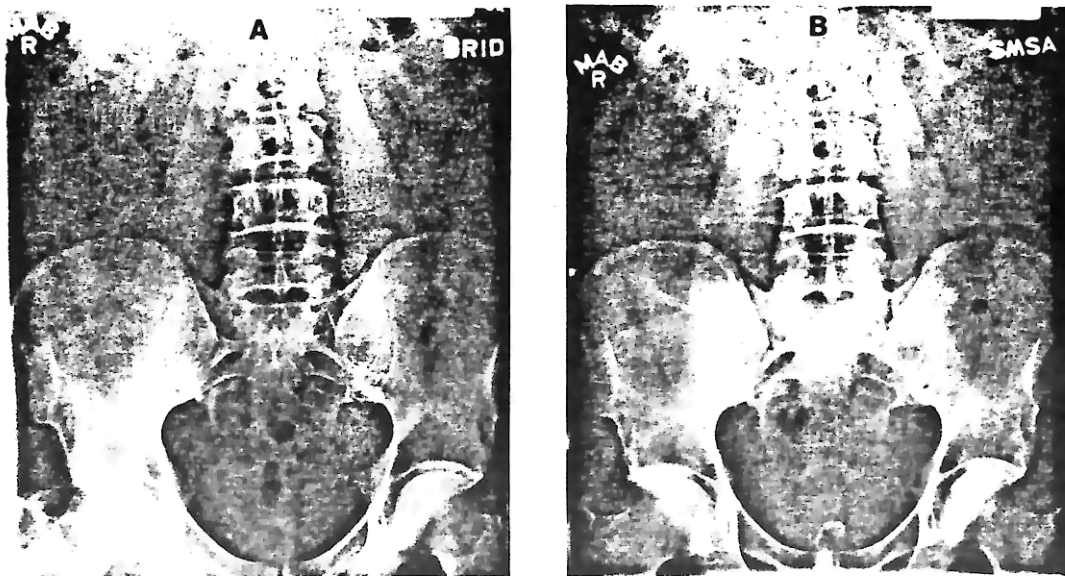


FIG. 13. Comparison AP abdominal radiographs illustrating the exposure reducing capability of SMSA. Subject measured 25 cm and radiation field was 36×43 cm: (a) 12:1, 40.6 lines/cm grid using 76 kVp (3 ϕ) and 600 mA at 0.15 s, 102 cm SID, 700 mR entrance skin exposure; (b) SMSA using 106 kVp (3 ϕ) and 600 mA at $\frac{1}{3}$ s, 122 cm SID, 255 mR entrance skin exposure. Both exposures were made employing a nominal 1.2 mm focal spot with same cassette using DuPont Hi Plus screens combined with Kodak RPL film. The films were developed within minutes of each other in the same processor. The same generator was employed for both films and the HVL's of the two source assemblies used were matched at 3.9 mm of Al at 80 kVp.

greatest with larger patients and at higher kVp's. This is due to the large percentage of scatter emerging from larger patients and the decrease in selectivity of grids relative to the SMSA at higher kVp's (see Fig. 11). At lower kVp's and with smaller patients the improvement in contrast is less marked. However, due to the poor primary transmission of grids relatively less patient exposure was required with the SMSA. The entrance skin exposure (ESE) of the SMSA varied from 60% to 140% of that of the grids studied at the same kVp to obtain films having matched overall densities.

It has been well documented in the literature that comparable images requiring less radiation can be obtained at higher x-ray tube voltages with a superior scatter reduction technique.^{19,25-28} An attempt was made to obtain images of comparable contrast by employing a 30 kVp higher technique with the SMSA. The results are illustrated in Fig. 13. Even at 30 kVp higher and $\sim 1/3$ the ESE the SMSA film has slightly more contrast and when compared side by side to the grid film it was judged to be diagnostically superior by radiologists. The patient in Fig. 13 had an upper abdominal measurement of 25 cm. Due to the dependence of scatter on patient size, the reduction in exposure that can be realized with the SMSA will also be patient size dependent. In addition, the reduction will be greater for lower and higher kVp ranges. The former because of the poor primary transmission of grids at lower kVp's and the latter because of their increased scatter transmission.

For radiographs at the same kVp the Bucky factor of the SMSA was from 3.3 to 9.5 times greater than that of the grid; whereas, for radiographs of comparable contrast (Fig. 13)

it was 2.3 times greater. This increased tube loading will undoubtedly decrease x-ray tube life in many instances. However, x-ray tubes used in general radiography when amortized over the number of exams performed during their life account for only a small fraction of the total exam cost.

IV. CONCLUSION

As demonstrated both quantitatively and qualitatively in the preceding sections, the SMSA can be used to great advantage when the beam emerging from the patient is mostly scatter, such as with large film radiographs of the abdomen. An alternative use of such a device would be in mammography, where scatter significantly degrades contrast^{29,30} and conventional grids cannot be used due to their poor transmission of low energy rays. As in abdominal radiography the SMSA could be exploited to produce images of superior quality at the same radiation exposure or equivalent images at substantially less radiation exposure than conventional techniques.

Applying Eq. (1) to the SMSA data in Table IV, one finds that slightly greater than 80% of the primary beam or possible contrast is imaged with the SMSA indicating that there is still room for improvement. As indicated in the design section, increased scatter reduction could be achieved with only a slight increase in tube loading with the SMSA by using the deeper aft slots. An alternative method of reducing scatter still further without significantly increasing the tube loading problem would be to scan the patient with wavy rather than linear slits.^{31,32}

ACKNOWLEDGMENTS

The authors would like to acknowledge the clinical trial contributions of Dr. Veronica L. Rouse and Dr. David M. Witten, the helpful discussions with H. Murray Cleare in the early states of the project, the machine shop work of Jerry R. Sewell, the help of Richard B. Gustafson on the generator interface, and the support and suggestions of the departmental service engineering staff, particularly William L. McDaniel and Dewey E. Narkates, throughout the development of the project. This work was supported in part by U.S. Public Health Research Contract N01-CB-53865 from the National Cancer Institute, National Institutes of Health.

^{a1}Current address, Department of Radiation Oncology, University of Alabama School of Medicine, Birmingham, Alabama 35233.

¹R. H. Morgan, Am. J. Roentgenol. 15, 67 (1946).

²H. E. Seeman and H. R. Spletstosser, Radiology 62, 575 (1954).

³J. G. Bonenkamp and W. H. Bolding, Acta Radiol. 55, 225 (1960).

⁴M. M. Ter Pogossian, M. E. Phelps, E. J. Hoffman, and J. O. Eichling, Radiology 113, 515 (1974).

⁵R. B. Wilsey, Radiology 23, 198 (1934).

⁶K. H. Reiss, Radiology 80, 663 (1963).

⁷G. T. Barnes, I. A. Brezovich, and D. M. Witten, Am. J. Roentgenol. 192, 497 (1977).

⁸In the literature the terms *slit* and *slot* are often used interchangeably. In this paper a distinction is made. A slit is a long narrow cut in a plate about 1.6 mm thick or less, whereas a slot is a similar cut in a much thicker piece of material.

⁹O. Pasche, Dtsch. Med. Wochenschr. 29, 266 (1903).

¹⁰L. G. Cole quoted by R. B. Wilsey, Am. J. Roentgenol. 8, 589 (1921).

¹¹F. A. Wahl, Roentgenpraxis 3, 855 (1931).

¹²A. Vallebona, *Trattato di Stratiografia* (Vallardi, Milano, Italy, 1952).

¹³G. Bucky, Method and apparatus for projecting roentgen images, U.S. Patent No. 1,164,987 (1915).

¹⁴H. E. Potter, Am. J. Roentgenol. 7, 292 (1920).

¹⁵G. T. Barnes and D. M. Witten, "Development and testing of a system to improve x-ray imaging, contrast and sharpness, while retaining the resolution of film." Contract proposal submitted to the National Cancer Institute for Research Funding Proposal No. NCI-CB-53865-33 (1974).

¹⁶C. Jaffe and E. W. Webster, Radiology 116, 631 (1975).

¹⁷G. T. Barnes, H. M. Cleare, and I. A. Brezovich, "Improvement of Contrast and/or Reduction of Patient Exposure in Diagnostic Radiology by Means of a Scanning Multiple Slit Assembly," in *Operational Health Physics, Proceedings of the Ninth Midyear Topical Symposium of the Health Physics Society*, edited by P. L. Carson, W. R. Hendee and D. C. Hunt (February 9-12, 1976, Denver, CO.), pp. 791-797.

¹⁸G. T. Barnes, H. M. Cleare and I. A. Brezovich, Radiology 120, 691 (1976).

¹⁹J. A. Sorenson and J. A. Nelson, Radiology 120, 705 (1976).

²⁰R. Moore, D. Korbuly, and K. Amplatz, Radiology 120, 713 (1976).

²¹Calculated for 3 ϕ generator from product data sheets for Eureka Sapphire X-Ray Tube with 12 $^\circ$ target and 10,000 rpm anode rotation, Eureka X-Ray Tube Co., Chicago, IL.

²²I. A. Brezovich and G. T. Barnes, "The Effect of Electron Evaporation on X-Ray Tube Current," in *Application of Optical Instrumentation in Medicine VI*, edited by J. E. Gray and W. R. Hendee, Proc. Soc. Photo Opt. Instrum. Eng. 127, 175 (1977).

²³E. D. Trout, D. E. Graves, and D. B. Slauson, Radiology 52, 669 (1949).

²⁴V. L. Rouse, D. M. Witten, and G. T. Barnes, to be published.

²⁵K. Lindblom, Acta Radiol. 36, 162 (1951).

²⁶F. Wachsman, K. Breuer, and E. Bachiem, Fortschr. Geb. Roentgenstr. 76, 147 (1952).

²⁷E. D. Trout, J. P. Kelley, and G. A. Cathey, Am. J. Roentgenol. 67, 946 (1952).

²⁸A. Nemet, W. P. Cox, and T. H. Hills, Br. J. Radiol. 26, 185 (1953).

²⁹G. T. Barnes and I. A. Brezovich, "Contrast: Effect of Scattered Radiation," in *Breast Carcinoma, The Radiologist's Expanded Role*, edited by W. W. Logan (Wiley, New York, 1977), pp. 73-81.

³⁰G. T. Barnes and I. A. Brezovich, Radiology 126, 243 (1978).

³¹Koch and Sterzel Aktiengesellschaft, Diaphragme á rayons secondaires pour rayons de Röntgen, French Patent No. 778,803 (1935).

³²I. A. Brezovich and G. T. Barnes, Med. Phys. 4, 451 (1977).

The Scanning Grid: A Novel and Effective Bucky Movement¹

Gary T. Barnes, Ph.D., Richard F. Moreland, Ph.D.,
Michael V. Yester, Ph.D., and David M. Witten, M.S., M.D.

A grid consisting of a focused array of radiopaque strips has been constructed. No interspace material is employed, and, during an exposure, the arrangement moves so that the grid strips remain focused and a uniform film density is obtained. Preliminary measurements and radiographs of patients indicate that such a device is a practical and effective method of suppressing scatter.

INDEX TERM: Radiography, instrumentation
Radiology 135:765-767, June 1980

The limitations of conventional Bucky grids in imaging thick body parts are well known and have recently led to the development of multiple slit devices (1-6). Alternatively, scatter suppression can be improved by employing a more efficient grid (7). In this paper, such a grid is discussed and compared to conventional Bucky grids.

METHOD

The grid (Fig. 1) consists of slats situated between the patient and the film. During an exposure, the slats scan the radiation field, and their motion is synchronized with the exposure time so that the film receives a uniform radiation exposure. Focusing is realized by the distance between slats provided by the lower slat spacer being the geometrical projection of the upper spacer distance. Both spacers are connected to a linkage arm which maintains focus and alignment during a scan. Such a grid has been constructed at the University of Alabama in Birmingham. Important design parameters are listed in TABLE I.

RESULTS

Preliminary evaluations of the scanning grid's primary and scatter transmission at 100 kVp are compared to commonly used grids (TABLE II). The details of the measurement techniques employed to obtain the data in TABLE II have been discussed previously (5, 8). These results indicate that the scanning grid is superior to commonly used grids. The primary transmission of the scanning grid is comparable to the lower ratio 8:1 grids, while its scatter transmission is markedly less than the 16:1 grid.

The contrast improvement obtained with an anti-scatter technique depends on the relative amount of scatter emerging from the patient and is given by

$$\text{Contrast Improvement} = \frac{SDF'}{SDF}, \quad (1)$$

where SDF' and SDF is the scatter degradation factor with and without the scatter reduction method (8-10). SDF is the fraction of the primary beam or possible contrast imaged due to the presence of scatter, and

$$SDF = (1 + S/P)^{-1}, \quad (2)$$

where S/P is the ratio of scattered-to-primary radiation imaged (10). Employing Equations 1 and 2 and the results tabulated in TABLE II, the contrast improvement obtained with the scanning

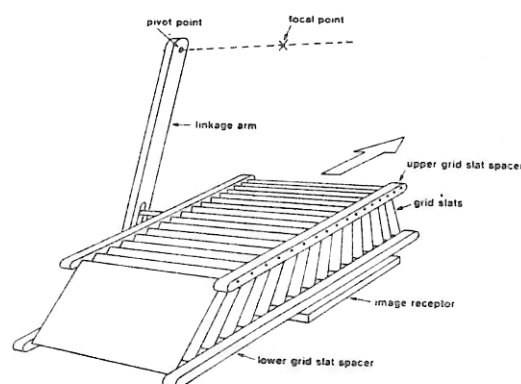


Fig. 1. *Diagram showing the principle of the scanning grid.

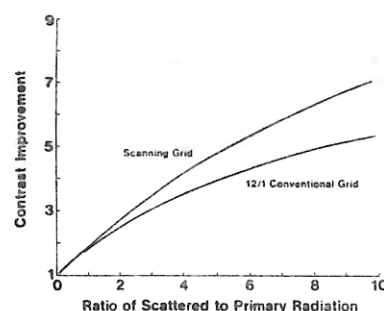


Fig. 2. Plot of the contrast improvement of the scanning and conventional 12:1 grid vs. the ratio of scattered-to-primary radiation emerging from the patient.

TABLE I: DESIGN PARAMETERS OF SCANNING GRID

SID*	122 cm	Septal thickness (lead)†	0.89 mm
Grid ratio	15.5/1	Septal thickness (total)‡	1.5 mm
Grid lines	1.64/cm	Septal height (lead)†	63.5 mm
Lead content	10.5 g/cm	Septal height (total)‡	71.5 mm
Magnification†	1.13		

* Source-to-image receptor distance

† At tabletop

‡ Lead septa are attached to steel substrate

TABLE II: COMPARISON OF THE PRIMARY AND SCATTER TRANSMISSION OF SCANNING AND COMMONLY USED GRIDS

Grid	% Primary Transmission*	% Scatter Transmission*
8/1, 31.5 lines/cm†	67	11.2
8/1, 41.3 lines/cm‡	66	11.4
12/1, 31.5 lines/cm†	60	6.4
16/1, 31.5 lines/cm†	56	4.2
Scanning grid	67	3.7

* Measured at 100 kVp (3φ), employing an 18-cm thick, 30-X 30-cm Lucite phantom

† Fiber interspace grids with lead contents of 363, 572, and 765 mg/cm²

‡ Aluminum interspace grid with a lead content of 360 mg/cm²

3a,b

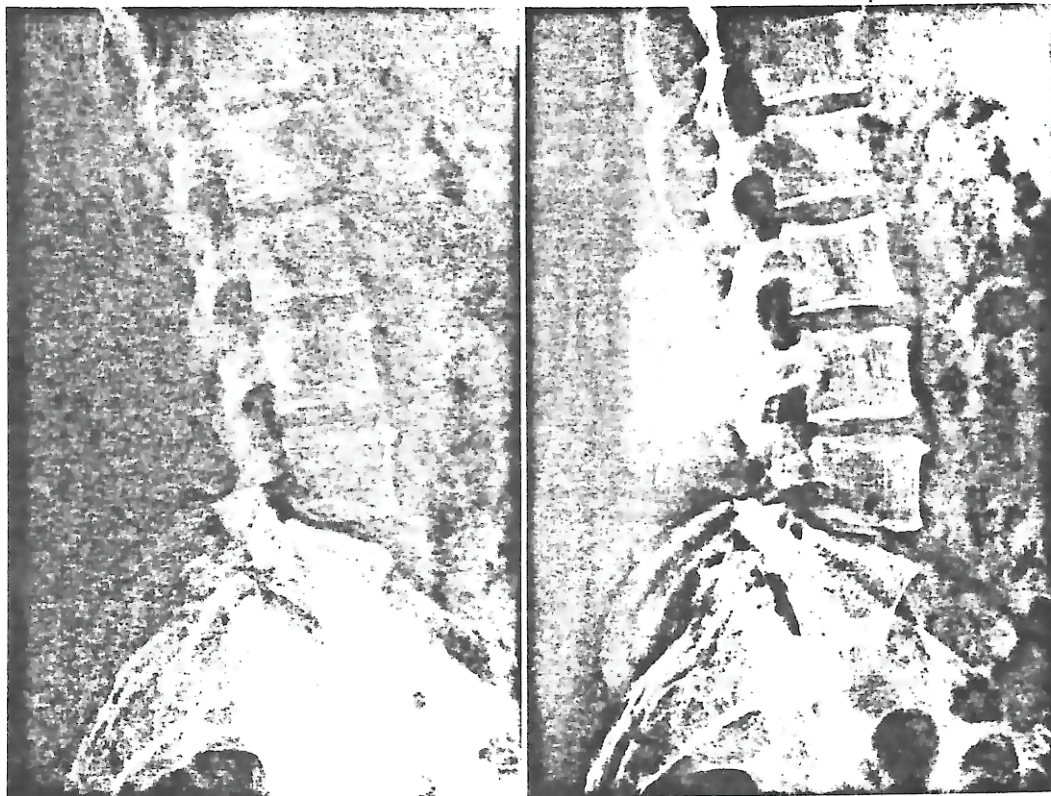


Fig. 3. Comparison of lateral lumbosacral spine radiographs at 100 kVp (3 ϕ). The radiation field was 23 X 43 cm. a. Twelve-to-one ratio, 31.5 lines/cm, fiber interspace grid using 100 mA at 0.8 sec., 102-cm source-to-image receptor distance, 2.2 R (0.57 mC/kg) entrance skin exposure, 1.4-mm focal spot size.

b. Scanning grid using 200 mA at 0.8 sec., 122-cm source-to-image receptor distance, 2.2 R (0.57 mC/kg) entrance skin exposure, 1.2-mm effective focal spot size.

Both exposures were made with the same cassette using Du Pont Hi Plus screens combined with Kodak X-Omatic L film. The radiographs were developed within minutes of each other in the same processor, and the half-value layers were matched at 3.5 mm Al at 80 kVp. The overall soft-tissue density of the conventional 12:1 grid film was greater than that of the scanning grid (1.6 vs. 1.2). Normalizing the film densities would have reduced the conventional grid entrance skin exposure by 30% to 1.5 R (0.39 mC/kg).

and commonly used grids as a function of S/P can be determined. This is plotted for the scanning and conventional 12:1 grid (Fig. 2) and illustrates that significant improvements in contrast over conventional grids should be obtained with the scanning grid for large S/P ratios.

The improvement in contrast achieved clinically by the scanning grid is illustrated in Figure 3. The patient is a 42-year-old man with a 33-cm lateral abdominal measurement. Figure 3a is a lateral radiograph of the lumbosacral spine made with a conventional 12:1 grid. Figure 3b is the same lateral projection made with the scanning grid at the same kilovolt peak and beam quality. The gross anatomic structures are seen on both radiographs. Abnormal findings include separation of the pars interarticularis at L-5, with associated sclerosis of the articular facets at the posterior articulations between L-4 and L-5 and small osteophytes anteriorly on several vertebral bodies. However, contrast is low on the conventional radiograph, but, with the

increase in contrast obtained on the scanning grid, the clarity of anatomic detail becomes markedly improved. Particularly notable are (a) the increased visibility of the abnormal findings, (b) the increased visibility of both the bony trabeculae and margins of the vertebra, and (c) the clarity of the adjacent soft-tissue structures.

A scanning grid is superior to a conventional grid because:

1. There is no scatter penetration of the relatively thick grid septa, and
2. There is no interspace material.

The lack of scatter septal penetration results in a decreased scatter transmission for a given grid ratio, while the air interspace results in a primary transmission that, for a given number of grid lines per centimeter, is independent of grid ratio. The current performance of the scanning grid could be improved by employing thinner lead septa (~ 0.1 – 0.2 mm), a higher grid ratio, and wavy or zigzag (7) rather than linear slats. Employing thinner

lead septa would increase the device's primary transmission, while the latter two modifications would decrease scatter transmission.

Linear tomography and angled views are accomplished with a conventional linear focused grid by moving the x-ray tube parallel to the grid lines. Such examinations can also be accomplished easily with a scanning grid, unlike multiple slit devices having comparable efficiency in suppressing scatter, by locating the linkage arm pivot along the line that passes through the focal spot and is parallel to the grid slats as depicted in Figure 1. Locating the pivot in such a manner maintains grid focus and alignment when the x-ray tube is moved.

CONCLUSIONS

Preliminary quantitative and qualitative results obtained with the scanning grid indicate that it is an effective and practical method of suppressing scatter. Furthermore, these results were obtained on the first clinical prototype built, and significant improvements are possible.

ACKNOWLEDGMENT: The authors gratefully acknowledge the design contributions and machine-shop work of Jerry R. Sewell.

REFERENCES

1. Barnes GT, Brezovich IA, Witten DM: Scanning multiple slit assembly: a practical and efficient device to reduce scatter. *AJR* 129:497-501, Sep 1977
2. Sorenson JA, Nelson JA, Niklason LT, et al: Rotating disk device for slit radiography of the chest. *Radiology* 134:227-231, Jan 1980
3. King MA, Barnes GT, Yester MV: A mammographic scanning multiple slit assembly—design considerations and preliminary results. [In] Logan WW, Muntz EP, eds: *Reduced Dose Mammography*. New York, Masson, 1979, pp 243-252
4. Rudin S: Fore-and-aft rotating wheel (RAW) device for improving radiographic contrast. [In] Grey J, ed: *Proceedings of the Society of Photo-Optical Instrumentation Engineers. Application of Optical Instrumentation in Medicine VII*. Bellingham, Wash., 1979, vol 173, pp 98-107
5. Barnes GT, Brezovich IA: The design and performance of a scanning multiple slit assembly. *Med Phys* 6:197-204, May-Jun 1979
6. Korbuly D, Moore R, Allen W, et al: Magnification rotational scanography: a comparison study. Presented at the Sixty-fifth Scientific Assembly and Annual Meeting of the Radiological Society of North America, Atlanta, Ga. Nov 25-30, 1979
7. Brezovich IA, Barnes GT: A new type of grid. *Med Phys* 4: 451-453, Sep-Oct 1977
8. Wagner RF, Barnes GT, Askins BS: The effect of reduced scatter on radiographic information content and patient exposure: a quantitative demonstration. *Med Phys* 7:13-18, Jan-Feb 1980
9. Bonenkamp JG, Boldingh WH: Quality and choice of Potter Bucky grids. I. A new method for the unambiguous determination of the quality of a grid. *Acta Radiol* 51:479-489, Jun 1959
10. Barnes GT, Cleare HM, Brezovich JA: Improvement of contrast and/or reduction of patient exposure in diagnostic radiology by means of a scanning multiple slit assembly. [In] Carson PL, Hendee WR, Hunt DC, eds: *Proceedings of the Ninth Midyear Symposium of the Health Physics Society*. Denver, Colo., Feb 9-14, 1976, pp 791-795

¹ From the Department of Diagnostic Radiology, University of Alabama School of Medicine, University of Alabama in Birmingham, Birmingham, Ala. Presented at the Sixty-fifth Scientific Assembly and Annual Meeting of the Radiological Society of North America, Atlanta, Ga., Nov. 25-30, 1979. Received Nov. 29, 1979 and accepted Jan. 18, 1980.

Effect of reduced scatter on radiographic information content and patient exposure: A quantitative demonstration^{a)}

Robert F. Wagner

Medical Physics Branch, Division of Electronic Products, Bureau of Radiological Health, Rockville, Maryland 20857

Gary T. Barnes

Department of Diagnostic Radiology, University of Alabama School of Medicine, Birmingham, Alabama 35233

Barbara S. Askins

Space Sciences Laboratories, National Aeronautics & Space Administration, Marshall Space Flight Center, MSFC, Alabama 35812

(Received 30 April 1979; accepted for publication 13 August 1979)

If a normal screen-film exposure is made using a conventional grid, a reduced exposure may be used with a superior scatter removal device to record the same image information. This theoretical conclusion is not readily demonstrated because of the limited visibility on the underexposed film. In this study radiographs underexposed by a factor of three with a scanning multiple slit assembly (SMSA) were enhanced autoradiographically and found visually to contain more information than properly exposed radiographs obtained under similar conditions using a conventional Bucky grid. This observation was confirmed by contrast scale and noise measurements. Furthermore, the entrance skin exposure of the radiograph using the SMSA was 45% of that required with the grid technique at the same beam quality.

I. INTRODUCTION

At a given kVp, a reduced image receptor exposure may be used with a superior scatter removal device to record the same or more image information than would result from a normal exposure using a standard Bucky grid. This point is generally neglected in studies with conventional screen-film systems where image contrast is emphasized rather than signal-to-noise ratio (SNR) analysis. With the advent of image processing and the capability to enhance contrast the latter type of analysis¹ is more meaningful. The purpose of this paper is to demonstrate these points and to verify experimentally—qualitatively and quantitatively—the results of theoretical predictions.

In Sec. II we present the elements of the SNR analysis for comparing two systems that differ only in their efficiency of scatter removal. The development leads to quantitative prescriptions for the relative patient and the relative image receptor exposures to obtain the same inherent information content (SNR) with the two systems. In Sec. III we describe an experiment in which a normally exposed image utilizing a grid technique is compared with an underexposed image obtained with a superior scatter removal device, the scanning multiple slit assembly (SMSA) of Barnes *et al.*²⁻⁵ The underexposed image was autoradiographically enhanced^{6,7} to improve the display and read-out of the information. Quantitative evaluation of both images is described in Sec. IV, and the results are compared with the theoretical predictions. Finally, in Sec. V we discuss immediate and future prospects for such applications of improved scatter removal technology.

II. BASIC THEORY

Ter-Pogossian⁸ indicated that scattered radiation serves as a noise generator in an imaging system. However, his analysis was limited to contrast alone. Analyses of signal-to-noise ratios (SNR) in the presence of scatter were performed by Muntz^{9,10} Wagner,^{11,12} Motz and Danos,¹ and Shaw¹³ among others. The straightforward application to low contrast images is sketched here.

Consider a lesion of projected area A which generates a signal count difference ΔP from the mean primary background level P in an equal area. The Rose model¹⁴ SNR is the ratio of the difference signal to the root mean square (rms) noise of the Poisson-distributed photon background over the area A , $P^{1/2}$, or

$$\text{SNR}_P = \Delta P / P^{1/2} = (\Delta P / P) P^{1/2}. \quad (1)$$

In Eq. (1) $\Delta P / P$ is commonly known as the primary beam subject contrast, C , of the lesion and $P^{-1/2}$ as the noise contrast, i.e., the contrast of the exposure fluctuations. If scatter is present with a uniform photon fluence of S/A , the SNR becomes

$$\text{SNR}_s = \Delta P / (P + S)^{1/2}, \quad (2)$$

and the subject contrast of the lesion is reduced to

$$C' = \Delta P / (P + S). \quad (3)$$

Defining the scatter degradation factor^{15,2} (SDF) equal to $(1 + S/P)^{-1}$, Eqs. (2) and (3) become

$$C' = C(\text{SDF}), \quad (4)$$

and

$$\text{SNR}_s = \text{SNR}_p \text{SDF}^{1/2}. \quad (5)$$

Equations (4) and (5) indicate that the SDF is the fraction of primary beam contrast imaged in the presence of scatter, and that scatter decreases the SNR by $\text{SDF}^{1/2}$.

If we introduce an antiscatter device having primary and scatter transmissions of T_p and T_s , the SNR becomes

$$\begin{aligned} \text{SNR}_a &= \Delta PT_p / (T_p P + T_s S)^{1/2} \\ &= \text{SNR}_p (\text{SDF}_a T_p)^{1/2}, \end{aligned} \quad (6)$$

where $\text{SDF}_a = [1 + T_s S / (T_p P)]^{-1}$. For an ideal device ($T_p = 1$, $T_s = 0$) operating at the same level of primary and scatter the SNR is equal to SNR_p as defined by Eq. (1).

The concept of detective quantum efficiency (DQE) was used by Wagner¹² to rank real antiscatter devices relative to an ideal device:

$$\text{DQE}_a = \text{SNR}_a^2 / \text{SNR}_p^2 = T_p \text{SDF}_a. \quad (7)$$

The definition relates to both devices operating at the same level of primary radiation, but depends only on the ratio of scatter-to-primary. (Generally, DQE of detectors is a function of primary exposure level; here as applied to scatter suppression it is independent of primary exposure.) DQE_a ranges from 0 (thick lead) to 1 (perfect grid). Using Eq. (6) to determine the relative primary exposure levels P_1 and P_2 for two different antiscatter techniques to yield equal SNR_s , one obtains

$$P_2/P_1 = \text{DQE}_1/\text{DQE}_2. \quad (8)$$

Since the beam qualities are assumed to be same in this treatment, the patient dose will scale the same way. When the reference device is ideal, Eq. (8) reduces to $1/\text{DQE}_2$ and gives the increase in patient dose required for the real device to achieve the same SNR that could be achieved by an ideal antiscatter grid. Equation (8) is a principal motivation for the definition of DQE. Here it ranks the exposure efficiency of a scatter reduction technique on the absolute scale established by the ideal grid. The history of DQE can be traced from A. Rose¹⁶ and R. C. Jones¹⁷ through Dainty and Shaw.¹⁸ Equations (7) & (8) are consistent with limiting cases in these references as well as Eq. (25) of Motz and Danos,¹ Eq. (16) of Dick and Motz,¹⁹ and Eq. (7.3) of Shaw,¹³ who treated a multistage process.

Finally, if one wishes to use the DQE advantage of one scatter removal device over another with the intention of maintaining a given SNR, one notes from rewriting Eq. (6) as

$$\text{SNR}_a = C_p \text{SDF}_a \cdot (T_p P + T_s S)^{1/2}, \quad (9)$$

that the relative image receptor exposures must be proportional to

$$\frac{(T_p P + T_s S)_2}{(T_p P + T_s S)_1} = \frac{\text{SDF}_1^2}{\text{SDF}_2^2} \quad (10)$$

This equation differs from a DQE ratio since it does not relate to radiation efficiency, only to film darkening or exposure at the image receptor.

TABLE I. Fundamental image parameters for scatter reduction devices used here.

Scatter reduction device	$T_s S / T_p P$ ratio	T_p	DQE
Grid	1.53 ± 0.14	0.66 ± 0.01	0.26
SMSA	0.27 ± 0.02	0.84 ± 0.01	0.66
None	7.3 ± 0.4	1.0	0.12

III. EXPERIMENTAL METHOD

The experiment reported here was designed to demonstrate the DQE patient exposure advantage that is calculated for the SMSA device over a conventional grid technique operating at the same beam quality. It involved making a series of radiographs of an imaging phantom using the grid technique with the proper exposure, and using the SMSA with an underexposure predicted by the above SNR analysis.

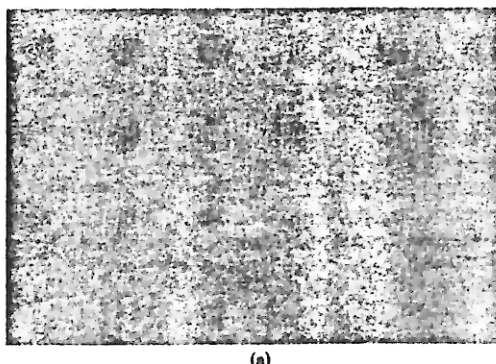
The phantom consisted of an epoxy resin base with a series of 1 cm diameter holes of varying depths (10% per step) filled with another epoxy resin with slightly less density and attenuation. The holes were tapered and beveled to reduce edge visibility. This inch-thick imaging phantom was embedded in the bottom of a $30 \times 30 \times 22$ cm thickness of a Lucite scattering phantom.

The values of the S/P ratio and T_p for the grid and SMSA with the scattering-imaging phantom described are listed in Table I. The S/P ratios were measured by placing a small lead beam stop centrally on the phantom. The x rays imaged beneath the beam stop are due to scatter, whereas beneath the rest of the phantom they are due to scatter plus primary. A film-screen combination was used as an image receptor and sensitometry was used to convert the densities obtained to relative exposure fluences. The details of the techniques employed have been described elsewhere.⁵ The primary transmission values tabulated in Table I were measured by placing the appropriate thickness of phantom material as close as possible to the x-ray tube, coning down to a small field and comparing the radiation with and without the grid or air slots.

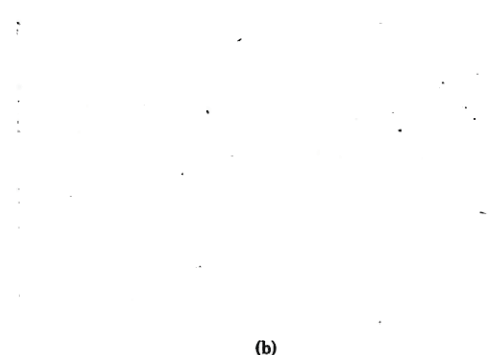
The DQE values given in the last column were calculated using Eq. (7) with the values of the scattering parameters of columns 2 and 3. The SMSA enjoys a DQE advantage of a factor 2.5 over the grid. Equation (10) indicates that the SMSA film can be underexposed by as much as a factor of four and still contain as much information as a properly exposed film obtained with the grid.

All radiographs were exposed using 100 kVp (3 phase, 12 pulse), the same (single) 3M alpha-8 screen, and Kodak Min-R film. This screen-film combination was selected for two reasons. First, the autoradiographic intensification technique (to be described below) is best suited to single emulsion films. Second, the bright phosphor of the screen and the fine grain of the film were insurance against film grain noise competing with x-ray quantum noise at the lower exposure used.

Radiographs were exposed to a gross density of 0.71 ± 0.02 with the grid and SMSA, and then a series of radiographs



(a)



(b)

FIG. 1. Comparison of normally exposed grid image (a) with underexposed SMSA image (b).

were exposed using the SMSA at 1/3 the exposure required for the "normal" (0.71 o.d.) image. In Fig. 1 the grid radiograph and an underexposed SMSA radiograph are compared. The density of the underexposed radiograph was 0.22, with at most four disks visible under any normal conditions of transillumination and 6 to 9 under scatter-illumination through the ends of the film. In order to determine the inherent information content of the underexposed film it was enhanced autoradiographically.

Autoradiographic intensification is a nuclear chemistry technique^{6,7} for retrieving the signal that has been recorded and stored in the emulsion at silver particle densities which are too low for easy visual or instrumental perception. The retrieval is accomplished by chemically combining the silver with radioactive sulfur-35 so that 0.167 MeV beta particles are steadily emitted from the low density image. The beta radiation is detected and recorded by making an autoradiograph of the activated original, i.e., by exposing a second film to the radiation from the original for about an hour and then developing this film by standard procedures. The original image is reproduced on the autoradiograph with increases in density and contrast that allow normal visual or instrumental evaluation of the signal. As used in this work the autoradiographic technique resulted in a contrast amplification of about a factor of 50.

The resulting intensified SMSA image is compared with the grid image in Fig. 2. Three rows of disks—a total of 18—are now visible. Attempts to intensify the grid image to such visibility were unsuccessful (16 or 17 visible). This demonstration was quantified using microdensitometric measurements of the image SNR's.

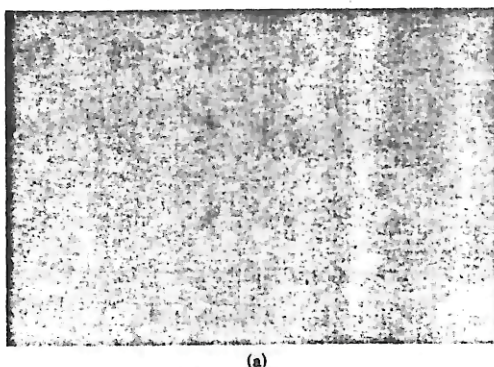
IV. IMAGING MEASUREMENTS

This experiment was designed to embrace only large area or low spatial frequency effects, i.e., to be free of questions concerning resolution. Large area information density is defined¹⁸ such that it is proportional (logarithmically or linearly, depending on the dynamic range of the application) to the large area SNR of Sec. II. The determination of this SNR requires two kinds of measurements, signal contrast $\Delta P/(P + S)$ and noise contrast $(P + S)^{-1/2}$.

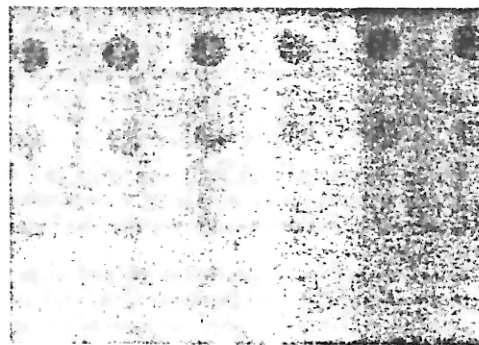
The signal contrast can be obtained by measuring the recorded density difference

$$\Delta D = (\log_{10} e) \gamma \Delta P / (P + S), \quad (11)$$

between the signal disk and the background. The product of γ , the contrast amplification factor of the screen-film system, and the logarithmic factor is of order unity,¹¹ and will in fact be regarded as unity here since we will only deal with ratios



(a)



(b)

FIG. 2. Comparison of normally exposed grid image (a) with autoradiographically enhanced SMSA underexposed image (b)

TABLE II. Results of contrast and noise measurements.

Autoradiograph film type	Gross density	Relative signal $\Delta D_S/\Delta D_g$	Relative noise*	SNR_S/SNR_G
M	1.28	5.93 ± 0.50	4.31 ± 0.32	1.38 ± 0.15
AA	0.60	2.48	1.89	1.31
R	0.50	2.51	2.02	1.24

*Low frequency noise spectrum amplitude

in which it drops out. Density differences were obtained by scanning across the center of the disk signals, and background trends were obtained by parallel scans through background alone using the PDS microdensitometer²¹ ($15 \times 600 \mu\text{m}$ postslit, 4X objective, N.A. 0.11). Background trends were normalized out in the determination of ΔD . Typical scans are given in Fig. 3. The lowest contrast results were on the grid film and range from 0.032 to 0.065 o.d.; the highest contrast results were on the type-M autoradiograph (AR) of the SMSA image and range from 0.229 to 0.336. The precision of all numbers that were differenced was better than 1%.

Results of the measurements on the first five holes of two grid images were averaged pairwise for comparison with the measurements on the first five holes of a high contrast SMSA/AR image. The ratio $\Delta D_S/\Delta D_g$, SMSA autoradiograph contrast to grid contrast was 5.93 ± 0.50 and is included in the summary of Table II.

The noise contrast $(P+S)^{-1/2}$, or the denominator of the SNR, is obtained from a measurement of the noise power (Wiener) spectrum W_D of the resulting screen-film noise. Following Shaw²⁰ we can define a noise equivalent number of quanta (NEQ) inferred from a film noise measurement

$$W_D(f) = (\log_{10} e)^2 \gamma^2 \text{MTF}^2 / \text{NEQ}, \quad (12)$$

where MTF is the screen-film modulation transfer function. This is simply a scaling of density fluctuations back to the exposure axis. As above we can set $\gamma \log_{10} e$ to unity. We note that since the film cannot distinguish the scatter from the primary contributions to NEQ, NEQ will be proportional to $S+P$. Since both images have the same limiting low frequency MTF we make the replacement

$$(P+S) = K/W_D(f \rightarrow 0), \quad (13)$$

where K will be of order unity, and will cancel approximately in the ratios below. In terms of the measurements described, the SNR becomes

$$\text{SNR} = K^{1/2} \Delta D / W_D^{1/2}(f \rightarrow 0). \quad (14)$$

Noise power spectra using the above optics (4.1 mm postslit) and the technique described in Ref. 22 were obtained for samples of all films used in this experiment. They are given in Fig. 4.

The power spectrum for the conventional grid image has the classical shape of filtered quantum mottle below about 6 mm^{-1} (i.e., 6 cycles/mm) upon a pedestal of film grain noise. The SMSA/AR films appear to be amplifications of this kind of noise in the low frequency region, followed by an

unsharp copy of the film grain, evident at frequencies greater than 8 mm^{-1} . The unsharpness is due to the 20–80 μm range of the beta's from the radioactive silver sulfide. The precision of these curves is about 8%. The repeatability (different samples) is about 10%. We use the values of W_D at 0.4, 0.8, 1.2, and 1.6 mm^{-1} as individual estimators of $W_D(f \rightarrow 0)$. These values are not particularly sensitive to the lowest frequency noise (trends) of film-coating and development variations. The average of ratios of $W_D^{1/2}$ for the SMSA to Grid image at the four low frequency points is shown in Table II.

The SMSA film underexposure factor of three leads to a theoretical patient underexposure factor of 1.9 on the basis of Eqs. (8)–(10), which assume no change in beam qualities. We measured a value of 2.2 for the patient exposure reduction. The larger measured value is attributed to a small increase in kVp (i.e., per cent transmission) that resulted with the lower mA station employed to obtain the underexposed film. The measurements lead to the theoretical estimate that the SMSA/AR SNR will be 1.16 that of the grid image. The ratio of SNR's from Eq. (14) and the image measurements is found to be 1.38 ± 0.15 and is given in the last column of Table II. We conclude that the SNR in the SMSA/AR film is significantly greater than that in the GRID film. Additional checks were obtained by a single disk contrast measurement and NPS measurement on SMSA/AR films made on AA and R film and the SNR ratios were found to fall within the range of variation of the more extensive measurements. The measurements support the visual impression that the SMSA/AR film contains slightly more information than the GRID film or the enhanced GRID film.

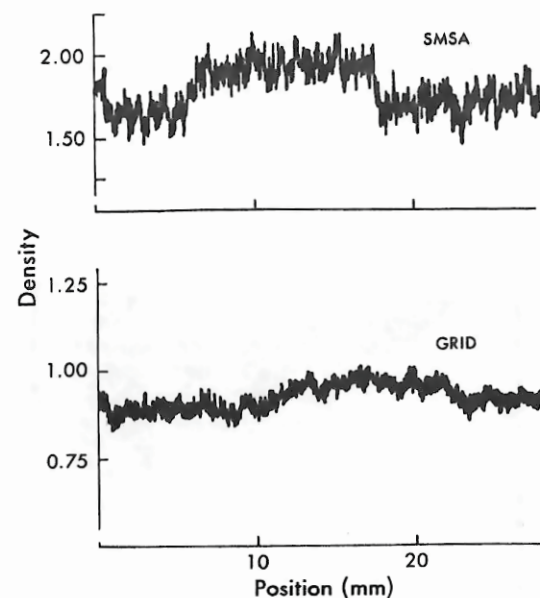


FIG. 3. Typical scans for determining contrast of grid image and SMSA image autoradiographs on type M, AA, and R film.

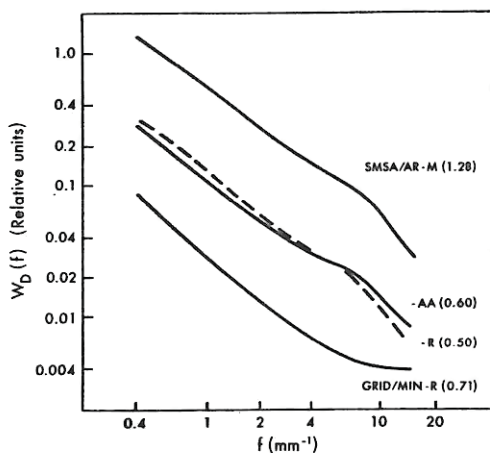


FIG. 4. Measured Wiener (noise power) spectra for grid image and SMSA image autoradiographs on type M, AA, and R film.

V. DISCUSSION AND CONCLUSIONS

It has been experimentally demonstrated, both qualitatively and quantitatively, that the theoretical DQE advantage of a superior scatter removal device can be used to decrease patient exposure without sacrifice in inherent image information content. Here the patient exposure reduction factor was 2.2, and the image made with the superior scatter removal device had, as predicted, a slight increase in SNR. An alternative method of reducing the SNR and patient exposure with a superior scatter removal device that has been well documented in the literature²⁻⁵ is to employ higher kVp techniques. This aspect is more difficult to accurately quantify and is not addressed in the present paper.

The autoradiographic intensification used to process the underexposed images in this study is not presently a commercially available process. Notwithstanding, the results reported here are immediately and practically realizable if the intensification is achieved through brighter phosphors or faster emulsions already commercially available. They were not used in the current study because of the limited speed selection available; the difficulty in matching the spectrum of primary x rays absorbed in the intensifying screen; and difficulties in interpreting the resultant noise power spectra shape differences.

As discussed in Refs. 12, 13, 16-18, a DQE advantage can be exploited either by maintaining SNR and decreasing exposure, or by maintaining exposure and increasing SNR. The recent introduction of rare-earth phosphors for intensifying screens represented an increase in DQE of up to a factor of two. This increase was used, for the most part, to reduce patient exposure.¹² The introduction of the SMSA represents an increase in DQE of about a factor of two for large body sections (and perhaps as much as a factor of 1.8 for mammography^{23,24}) and can be used to either advantage.

In addition to the possibilities for exposure reduction previously discussed (and excluding questions of resolution), there is also the possibility of optimizing the x-ray spec-

trum—an area of growing theoretical interest, but little practical experimental demonstration due in part to the limited exposure latitude of film. We believe that autoradiographic intensification has immediate applications in this area, for testing the theory and preparing for future advances in image recording and processing modalities.

Finally, the use of the autoradiographic technique shows dramatically the possible large amount of information recorded on film that is not effectively displayed by ordinary processing. Recall the emphasis of Motz and Danos¹ that unless the reader runs up against noise as a limitation to his reading, he is not exhausting the information in the image. In practice, contrast limitations to film reading are more common than noise limitations; the signal that information on the film has been exhausted is not frequently received. In this light, our study is another documentation of the need for an image display modality without the display limitations of film.²⁵

ACKNOWLEDGMENTS

GTB acknowledges discussions with H. Murray Cleare, and GTB and RFW acknowledge discussions with Roger H. Schneider before this work was begun. We thank Earl W. Denny and James E. Duff for designing and fabricating the phantom used in this work. RFW is grateful to John Sandrik for developing the long slit noise power spectrum software.

²⁵Presented at Twentieth Annual Meeting of the American Association of Physicists in Medicine, San Francisco CA, August 1978.

¹J. W. Motz and M. Danos, *Med. Phys.* **5**, 8 (1978).

²G. T. Barnes, H. M. Cleare, and I. A. Brezovich, in *Proc. Ninth Midyear Symp. Health Phys. Soc.*, edited by P. L. Carson, W. P. Hendee, and D. C. Hunt, Denver, Colorado, February 1976, pp. 791-795.

³G. T. Barnes, H. M. Cleare, and I. A. Brezovich, *Radiology* **120**, 691 (1976).

⁴G. T. Barnes, I. A. Brezovich and D. M. Witten, *Am. J. Roentgenol.* **129**, 497 (1977).

⁵G. T. Barnes and I. A. Brezovich, *Med. Phys.* **6**, 197 (1979).

⁶B. S. Askins, *Appl. Opt.* **15**, 2860 (1976).

⁷B. S. Askins, *Science* **199**, 684 (1978). Also, National Aeronautics and Space Administration: U.S. Patent No. 4101780. (A detailed protocol for the autoradiography technique may be obtained by requesting Technology Brief No. MFS-23461 from the Technology Utilization Office, Marshall Space Flight Center, AL 35812).

⁸M. M. Ter-Pogossian, *The Physical Aspects of Diagnostic Radiology* (Hoeber, New York, 1967).

⁹E. P. Muntz and M. S. Welkowsky, in *Breast Carcinoma: The radiologists Expanded Role*, edited by W. W. Logan (Wiley, New York, 1977), pp. 207-217.

¹⁰E. P. Muntz, M. Welkowsky, E. Kaegi, L. Morsell, E. Wilkinson, and G. Jacobson, *Radiology* **127**, 517 (1978).

¹¹R. F. Wagner, *Med. Phys.* **4**, 279 (1977).

¹²R. F. Wagner, *Photogr. Sci. and Eng.* **21**, 252 (1978).

¹³R. Shaw, *Rep. Prog. Phys.* **41**, 1103 (1978).

¹⁴A. Rose, *J. Opt. Soc. Am.* **38**, 196 (1948). In Ref. 1, the noise is $(2P)^{1/2}$ since the noise in the background is correctly included. In the Rose model the noise is $(P)^{1/2}$, and the background noise is ignored. The difference will show up in the required value of the SNR at threshold (see Ref. 11).

¹⁵R. H. Morgan, *Am. J. Roentgenol.* **15**, 67 (1946).

¹⁶A. Rose, *J. Soc. Motion Pict. Eng.* **47**, 273 (1946).

¹⁷R. C. Jones, in *Advances in Electronics and Electron Physics* **X1**, edited by L. Marton (Academic, New York, 1959), pp. 87-183.

¹⁸J. C. Dainty and R. Shaw, *Image Science* (Academic, New York, 1974).

Wagner, Barnes, and Askins: Effect of reduced scatter

¹⁹C. E. Dick and J. W. Motz, *Med. Phys.* **5**, 133 (1978).

²⁰R. Shaw, *Opt. Acta* **20**, 749 (1974).

²¹Perkin-Elmer Corporation, Pasadena, CA.

²²R. F. Wagner, *Med. Phys.* **4**, 157 (1977).

²³G. T. Barnes and I. A. Brezovich, in *Breast Carcinoma: The Radiologist's Expanded Role*, edited by W. W. Logan (Wiley, New York, 1977), pp. 73-81.

²⁴G. T. Barnes, in *Reduced Dose Mammography* ed. by W. W. Logan and

E. P. Muntz (Masson, New York), 1979, pp. 223-242.

²⁵Problems encountered in the routine use of autoradiographic intensification include time, cost, and disposal of radioactive solutions. At least 10 min of activation time are required to activate the silver and another 30 min to 1 h are required for pre and post rinses; then the film must be dried prior to the autoradiograph exposure which requires a minimum of 1 h. The present cost to activate one 8 × 10 in film is approximately \$15.00 and the lowest estimate for routine usage is \$2.00 per 8 × 10 in. film.

Experimental measurements of the scatter reduction obtained in mammography with a scanning multiple slit assembly^{a)}

Michael V. Yester, Gary T. Barnes, and Michael A. King^{b)}

Department of Diagnostic Radiology, University of Alabama School of Medicine, The University of Alabama in Birmingham, Birmingham, Alabama 35294

(Received 28 July 1980; accepted for publication 6 November 1980)

A nonconventional and sensitive method of measuring scatter is described. The method was employed to quantitate the scatter imaged in mammography with a conventional unit, a unit equipped with a grid, and a unit equipped with a scanning multiple slit assembly (SMSA). The results indicate that the grid technique significantly reduces the scatter imaged, while the SMSA virtually eliminates it. The resultant increase in large area contrast is readily apparent on radiographs with greater improvement obtained with the SMSA than with the grid. The effect of the increase in contrast on small detail visibility was assessed with a phantom having simulated fibrils and calcifications. Significantly more fibril and calcification detail was visible with the grid and SMSA technique than with the conventional technique. The detail visible with the grid and SMSA technique was comparable, and the lack of better performance by the SMSA unit is attributed to its poorer MTF.

Key words: mammography, grids, scattered radiation

INTRODUCTION

It is well known that scatter radiation reduces visual contrast in a radiographic image. This is true in mammography as well, and in fact, the scatter-to-primary (s/p) ratio for this modality ranges from 0.35–1.0.¹ Consequently, only 75%–50% of the possible subject contrast is imaged, and improvements from 35%–100% are possible if scatter is eliminated. In order to reduce the scatter to a minimal level, a Scanning Multiple Slit Assembly (SMSA) was designed for mammography,² and three major investigations were carried out to test its performance: (1) measurement of transmitted scatter-to-primary ratios, (2) use of the mammographic phantom designed by Stanton *et al.*,³ and (3) clinical trials. The first and second investigations are the interest of this paper and were carried out for a conventional unit, the SMSA, and the conventional unit equipped with a special soft tissue grid.⁴ The results of the clinical trials have been presented elsewhere.^{5,6}

PRINCIPLE OF SMSA

Although the principle and construction of the device has been presented elsewhere,² a short description is given here for completeness and orientation. The underlying concept is that through the use of an array of long narrow x-ray beams, the volume irradiated at any given instant is small, thus reducing the production of scatter. With the long narrow geometry, little of the scatter produced by a beam reaches the image plane in the area defined by the beam and scatter from neighboring beams is minimized by post patient collimation. In the SMSA, slits between the source and the patient define the array of long narrow beams, and the post

patient collimation is accomplished with slots between the patient and film. The slits and slots are aligned with the x-ray source and scan synchronously across the patient during the exposure as shown schematically in Fig. 1. The design was incorporated into a commercial mammographic unit,² and was based on previous experience with a unit used for abdominal radiography.⁷

EXPERIMENTAL MEASUREMENTS

Experimental method for s/p measurements

Typically s/p measurements are performed using a lead beam stop at the center and above a suitable scattering medium. The radiation emerging from the phantom beneath the beam stop is scatter, and radiation at other points of the phantom is scatter plus primary. To accurately measure the percentage of scatter imaged, it is desirable to perform the measurements with the same detection system as used under clinical conditions. For the SMSA, the expected s/p value was ~ 0.03 ,² which implies that a dynamic range for the detector response of $\sim 30:1$ would be required for the usual measurement technique. Such a dynamic range is beyond the capabilities of commonly used film/screen combinations. Detectors having a greater dynamic range such as NaI-(Tl)/photomultiplier systems could be employed, but they have a different energy response than the film/screen combination. Such systematic errors can be avoided by employing a film/screen system if the measurement technique is changed.

In order to measure the expected low s/p ratios with a film/screen system, a lower contrast object (aluminum disk)

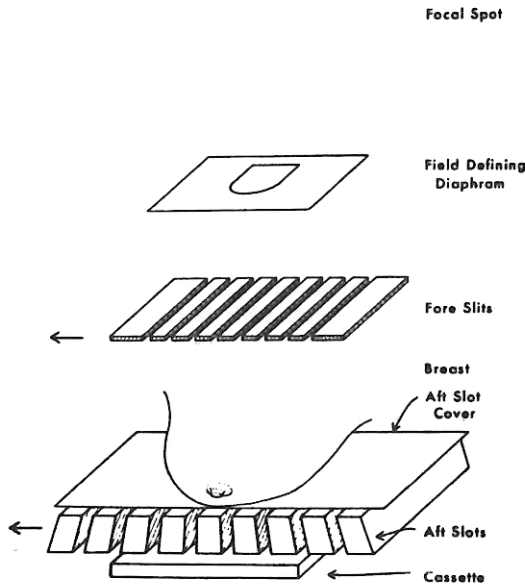


FIG. 1. Principle of mammographic SMSA.

was employed in place of the lead beam stop. Consider the fundamental equation for the imaged contrast of an object in the presence of scatter:

$$\Delta D = \bar{\gamma} \log \left[\frac{p + s}{o + s'} \right], \quad (1)$$

where ΔD is the density difference (image contrast) between the test object and surrounding area, $\bar{\gamma}$ is the slope of the film's sensitometric curve between the densities of interest, p and s are the primary scatter energy fluences absorbed in the screen adjacent to the object image, and o and s' are similar fluences associated with the object image.

For small objects, it is usually assumed that the scatter associated with the object image is equal to the scatter at adjacent locations. That is, s' is equal to s and Eq. (1) reduces to

$$\Delta D = \bar{\gamma} \log \left[\frac{p + s}{o + s} \right] \quad (2)$$

Solving for s/p , one obtains

$$\frac{s}{p} = \frac{1 - (o/p) 10^{(\Delta D/\bar{\gamma})}}{10^{(\Delta D/\bar{\gamma})} - 1} \quad (3)$$

Theoretically, for a given $\bar{\gamma}$ and permissible ΔD , s/p ratios arbitrarily close to zero can be measured for appropriate values of o/p . In practice, o/p is selected so that the range of s/p ratios anticipated can be measured to a reasonable degree of precision. Note that utilizing the linear portion of a typical mammographic sensitometric curve ($\Delta D \sim 1.0$ and $\bar{\gamma} \sim 2.2$), the minimum s/p ratio that can be measured with a lead beam stop ($o/p = 0$) is 0.54, and if the entire useful range of densities is employed ($\Delta D \sim 1.75$ and $\bar{\gamma} \sim 2.0$), the minimum s/p ratio that could be measured is 0.15.

Medical Physics, Vol. 8, No. 2, Mar./Apr. 1981

Measurements of s/p

In view of the preceding discussion, Al (alloy 1101) disks of 1 mm thickness and diameters of 0.5, 0.8, 1.0, and 2.0 cm were fabricated. The multiple diameters were employed to enable extrapolation of the data to "zero" size, thereby assuring that the assumption of $s' = s$ is valid.

In order to obtain $\bar{\gamma}$ over the range of densities of interest, sensitometric curves were generated experimentally for the particular emulsion number, film/screen combination, and processor used. This was accomplished using a kVp "bootstrap" technique as discussed elsewhere.⁸ Experimental studies have shown good agreement between kVp "bootstrap" and inverse square sensitometry over the useful range of densities as long as the former method is corrected for reciprocity failure.⁹ The agreement is particularly good over the straight line region of the sensitometric curve and this region was used exclusively in this work. A typical sensitometric curve obtained with this method is given in Fig. 2.

A 14 cm diameter Lucite phantom was employed and the scatter-to-primary ratios were measured for a 3 and a 6 cm thickness at 30 and 39 kVp (1 ϕ), respectively. In all cases, a molybdenum-tungsten alloy target x-ray tube¹⁰ and molybdenum filter (30 μ m) was employed. In order to obtain the s/p ratio, the object-to-primary ratio had to be determined for each configuration. This was accomplished by collimating the beam to a small, well-defined area (0.5 cm²), introducing a 15 cm air gap, and obtaining the optical density for a particular phantom thickness with and without the aluminum. The o/p ratio for each condition was obtained from the expression:

$$o/p = 10^{(\Delta D/\bar{\gamma})}. \quad (4)$$

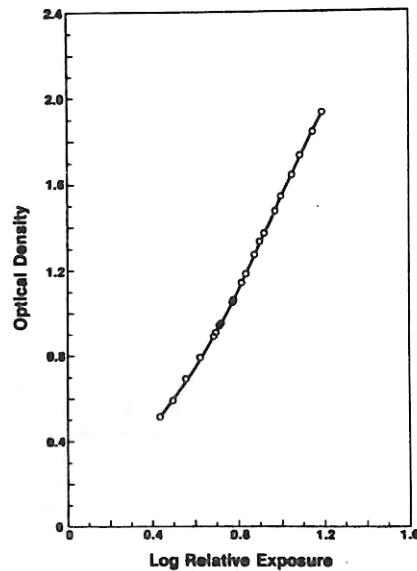


FIG. 2. Typical kilovoltage bootstrap sensitometric curve obtained with a Kodak min-R film/screen combination. The curve has been corrected for the small reciprocity failure that occurred over the factor of two difference in exposure times (0.25 to 0.5 s) employed to generate the curve.

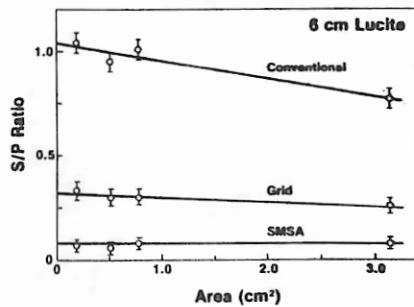


FIG. 3. Plot of the ratio of scatter-to-primary radiation measured for the conventional unit, the unit equipped with a grid and the SMSA as a function of aluminum disk area. The Lucite phantom was 14 cm in diameter and 6 cm thick.

The experimental procedure followed for the s/p measurements consisted of making an exposure with the four Al disks symmetric about and near the center of a Lucite phantom. Values for the change in density (ΔD) from the center of the disk to the region outside of the disk was obtained by averaging four values at 90° , with respect to each other around and just outside the disk. The density at the center of the disk was subtracted out to obtain the density difference (ΔD). The same measurements were performed for the conventional unit, the SMSA, and the conventional unit with a special grid.⁴ In this latter case, the grid was supported above the film cassette in such a manner to permit oscillations in one dimension parallel to the film to remove grid lines from the images. Three separate runs were made for the three cases to minimize random errors.

Phantom measurements

In addition to s/p measurements, a phantom was used to assess detail visibility of simulated anatomical features present in mammographic exams. The phantom used is that described by Stanton *et al.*³ and consists of polyethylene slabs of water-filled containers of differing thicknesses to simulate breast compositions of different water/fat ratios. Calcifications are simulated by the use of Al specks and different sizes are included in the phantom. Fibrils are simulated by the use of acrylic rods in an organic oil medium. For this work, the phantom was set up to imitate a composition of a ratio of 50/50 water/fat by volume for a total thickness of 4.7 cm. The phantom was imaged with the three modalities under consideration at 36 kVp with the mAs varied such that an optical density of approximately 1.2 was obtained. A Kodak Min-R film/screen combination was used as before.

TABLE I. s/p Ratios for conventional, grid and SMSA techniques.^{a)}

	3 cm, 30 kVp	6 cm, 39 kVp
Conventional	0.40 ± 0.05	1.04 ± 0.15
Grid	0.14 ± 0.03	0.32 ± 0.06
SMSA	0.05 ± 0.02	0.08 ± 0.04

^{a)} errors are based on propagation of uncertainties.

TABLE II. Error propagation trends.^{a)}

$\bar{\gamma}$	σ/p	ΔD	s/p
2.14	0.60	0.20	1.07
2.09	0.60	0.20	1.02
2.14	<u>0.63</u>	0.20	0.91
2.14	0.60	<u>0.215</u>	0.94
2.14	0.60	0.43	0.08
2.09	0.60	0.43	0.06
2.14	<u>0.63</u>	0.43	0.00
2.14	0.60	<u>0.445</u>	0.05

^{a)} The underlined quantity indicates the parameter that was changed. The difference in the parameters represents typical experimental uncertainties.

RESULTS

The data and s/p ratios obtained for the three cases are given in Table I, and the results for the 6 cm phantom are presented graphically in Fig. 3. In such an experimental technique with calculations involving exponents and small differences, it is necessary that the propagation of uncertainties are taken into account. As the measured s/p ratio depends on ΔD , σ/p and $\bar{\gamma}$, then it is necessary to understand which components have the greatest effect on the result. This was accomplished by obtaining the equation for the uncertainty in s/p as a function of the three parameters and their individual uncertainties in the usual error analysis manner. The actual equation obtained is quite complex and not readily amenable to quick insights into the error propagation. In order to provide perhaps a more meaningful appreciation of the problem, the components of the s/p uncertainty are given in Table II for two representative measurements, a high s/p ratio and a low s/p ratio. The uncertainties given in Table II were calculated from the derived formula.

The images obtained with the Stanton phantom are presented in Fig. 4. The detail visibility was determined³ for each film for the specks and fibrils, and the results are summarized in Table III.

DISCUSSION AND CONCLUSIONS

A new method for measuring s/p ratios has been described. It should be noted that the method is not limited to mammography, rather it is particularly suited for any situation involving small amounts of scatter. The method can be employed to quantitate the amount of scatter imaged whenever a film/screen combination is used as an image receptor. As mentioned previously, the subject contrast of the disks can be varied so that s/p ratios arbitrarily close to zero can be measured for a given film/screen dynamic range.

Previously reported s/p ratios for 3 and 6 cm thicknesses

TABLE III. Detail visibility results.

	Minimum fibril size (mm)	Minimum speck size (mm)
Conventional	0.3	0.23
Grid	0.25	0.18
SMSA	0.25	0.18

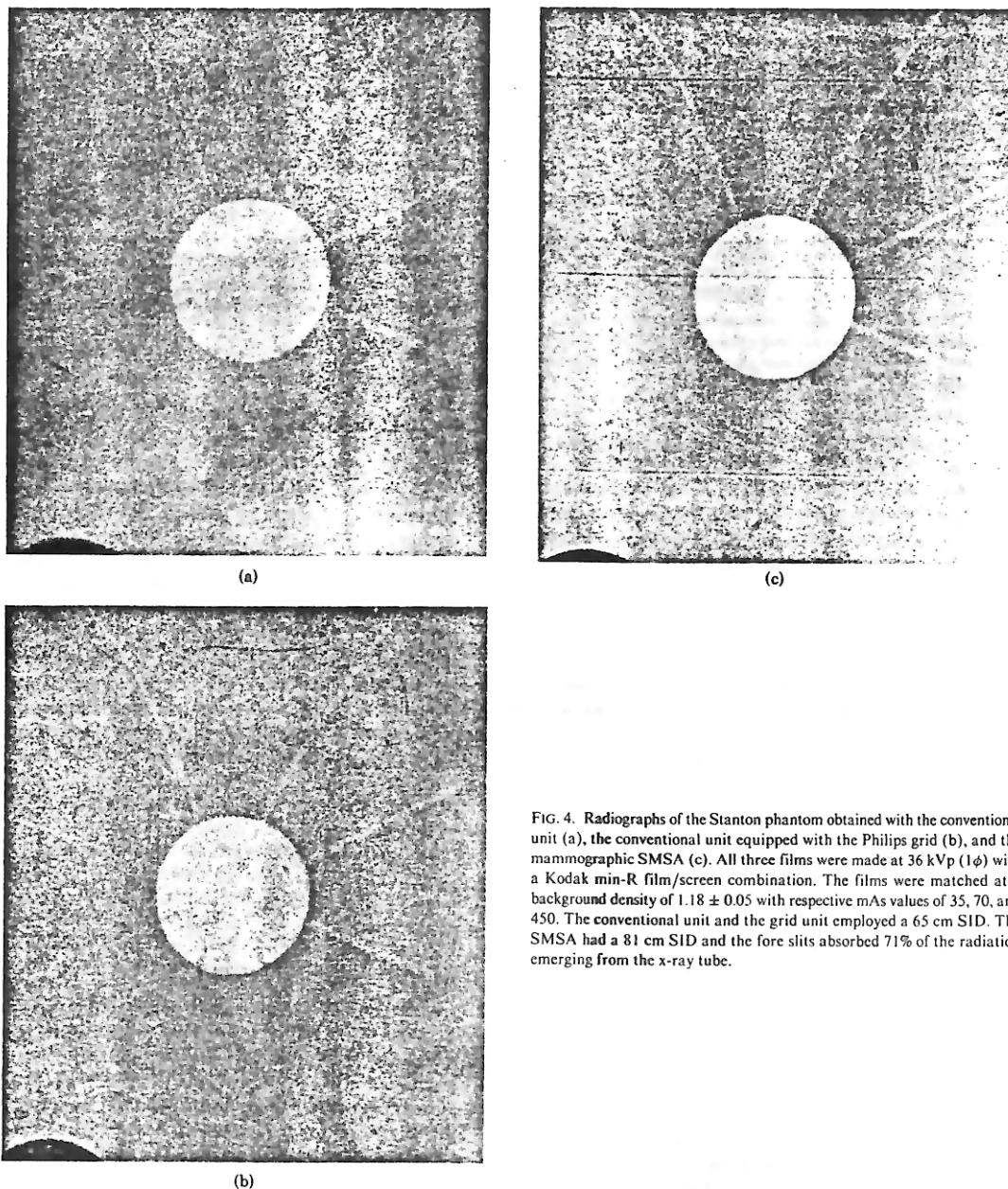


FIG. 4. Radiographs of the Stanton phantom obtained with the conventional unit (a), the conventional unit equipped with the Philips grid (b), and the mammographic SMSA (c). All three films were made at 36 kVp (1 ϕ) with a Kodak min-R film/screen combination. The films were matched at a background density of 1.18 ± 0.05 with respective mAs values of 35, 70, and 450. The conventional unit and the grid unit employed a 65 cm SID. The SMSA had a 81 cm SID and the fore slits absorbed 71% of the radiation emerging from the x-ray tube.

of a 14 cm diameter Lucite phantom were 0.40 and 0.85.^{11,12} The agreement with the results for the conventional unit and 3 cm phantom thickness is exceptionally good. For the 6 cm phantom thickness, there is a difference between the two measurements. Since a NaI(Tl) crystal/photomultiplier system was employed previously, this difference can be attributed in part to the difference in the energy responses of the film/screen combination and NaI(Tl) crystal.¹ The different responses would give rise to a greater difference in

the s/p ratios for thicker phantoms (i.e., 6 cm) where there is a greater shift in energy between the scattered and primary x-rays.

For the grid and SMSA s/p measurements, several features are noteworthy. The SMSA does indeed reduce the scatter significantly, and to the degree expected. The grid also reduces scatter, but not as effectively as the SMSA. Also of importance for antiscatter devices is their primary transmission. For the SMSA, the primary transmission is 0.72 at

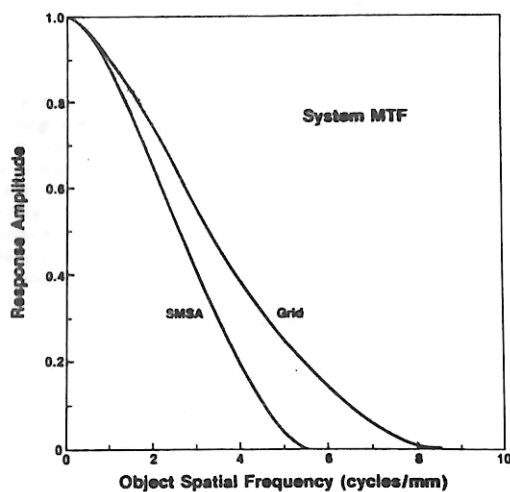


FIG. 5. Plot of the system MTFs at the object plane of the Stanton phantom for the grid unit and SMSA. The conventional unit had the same object magnification factor and focal spot size (and therefore system MTF) as the grid unit. The focal spot MTF was calculated employing a rectangular model which has been shown by Burgess to agree well with experimentally determined MTFs for spatial frequencies up to the first minimum.¹³ The min-R film/screen MTF employed for the calculation was measured by Gary K. Sanderson of Eastman Kodak Co.¹⁴

30 kVp and 0.74 at 39 kVp as compared to 0.61 and 0.65 for the grid at the respective kVp's and thicknesses of Lucite. The primary transmission for the SMSA is lower than expected. This occurred because the focal spot size was larger than anticipated (1.8 mm rather than 1.0 mm) which resulted in the fore slit x-ray projections spreading beyond the aft slot area.

In addition, there is an obvious decrease of the *s/p* ratio observed as a function of increasing size of the disks for the conventional unit and to a lesser degree when the grid is used (see Fig. 3). For the SMSA, however, the ratio is constant within experimental uncertainties over the range of diameters used. This indicates that the SMSA virtually eliminates all of the scattered radiation.

Of equal importance is the performance of the SMSA in regards to a detail visibility study. In the images obtained with the Stanton phantom, the grid performed equally as well as the SMSA in regard to detail visibility, although as can be seen in Fig. 4 the film taken with the SMSA does have greater large area contrast. In making this comparison of detail visibility it is necessary, though, to consider the geometrical magnification and system MTF. It was necessary to increase the object to film distance for the SMSA in order to put in the aft slots. This resulted in a magnification of 1.11 for the SMSA as compared to 1.06 for the grid. As the focal spot size of the tube measured with a star test pattern was 1.8 mm, the increase in magnification results in a definite loss

of resolution. To demonstrate this, the MTF for both the grid unit and the SMSA was calculated and the results are plotted in Fig. 5. The difference is substantial and it is noteworthy that the greater contrast achieved with the SMSA compensated for its poorer MTF and resulted in small detail visibility comparable to that obtained with the unit equipped with the grid. Employing a smaller focal spot would improve the SMSA's small detail visibility and in the near future a 0.4 mm focal spot will be incorporated into the unit. Another improvement that is planned is to replace the current 1.6 mm thick Lucite breast support cover with a 0.6 mm thickness of carbon fibre (a 0.75 mm carbon fibre support cover was employed for the grid *s/p* and primary transmission measurements). It is anticipated that the carbon fibre support cover along with the 0.4 mm focal spot will increase the SMSA's primary transmission to 90%–95%.

ACKNOWLEDGMENT

The authors would like to thank Leonard Stanton for the loan of his phantom that made the detail visibility measurements possible.

^{a1}Presented at the Twenty-First Annual Meeting of the American Association of Physicists in Medicine, Atlanta, GA, August 1979.

^{b1}Current address: Department of Nuclear Medicine, University of Massachusetts Medical Center, Worcester, Massachusetts.

¹G. T. Barnes, in *Reduced Dose Mammography*, edited by W. W. Logan and E. P. Muntz (Masson, New York, 1979), pp. 223–242.

²M. A. King, G. T. Barnes, and M. V. Yester, in *Reduced Dose Mammography*, edited by W. W. Logan and E. P. Muntz (Masson, New York, 1979), pp. 243–252.

³L. Stanton, T. Villafana, J. L. Day, and D. A. Lightfoot, *Invest. Radiol.* **13**, 291 (1978).

⁴The grid has a 5:1 ratio, 32 lines/cm, a lead content of 55 mg/cm² and is available from Phillips Medical Systems Inc., Shelton, CT.

⁵D. E. Hogg, A. K. Tonkin, and G. T. Barnes, "Improved image quality or reduced exposure in mammography by use of a scanning multiple slit assembly," Paper 11, 64th Scientific Assembly and Annual Meeting of the Radiological Society of North America, Chicago, IL, November 1978.

⁶A. K. Tonkin, D. E. Hogg, G. T. Barnes, M. V. Yester, and M. A. King, "Minimum dose mammography: Clinical application of the scanning multiple slit assembly (SMSA)," Scientific exhibit, 64th Scientific Assembly and Annual Meeting of the Radiological Society of North America, Chicago, IL, November 1978.

⁷G. T. Barnes and I. A. Brezovich, *Med. Phys.* **6**, 197 (1979).

⁸M. V. Yester, G. T. Barnes, and M. A. King, *Radiology* **136**, 785 (1980).

⁹L. K. Wagner, A. G. Haus, G. T. Barnes, J. A. Bencomo, and S. R. Amtey, *Proc. Soc. Photo-Opt. Instrum. Eng.* **233**, 7 (1980).

¹⁰Model D0069B X-Ray Tube Insert, General Electric Medical Systems, Milwaukee, WI.

¹¹G. T. Barnes and I. A. Brezovich, in *Breast Carcinoma: The Radiologist's Expanded Role*, edited by W. W. Logan (Wiley, New York, 1977), pp. 73–81.

¹²G. T. Barnes and I. A. Brezovich, *Radiology* **126**, 243 (1978).

¹³A. E. Burgess, *Invest. Radiol.* **12**, 44 (1977).

¹⁴G. T. Barnes, in *The Physics of Medical Imaging: Recording System Measurements and Techniques*, edited by A. H. Haus (Am. Inst. of Phys., New York, 1979), pp. 148–149.

Image Quality: An Educational and Scientific Problem¹

Gary T. Barnes, Ph.D.
David M. Witten, M.S., M.D.

The preceding Opinion is discussed, and a contrasting view presented. It is argued that image quality standards do exist; however, human, chemical, and mechanical factors cause image degradation. This problem cannot be solved by committee-derived standards but may be improved by educating radiologists as to the effects of changing various performance parameters.

Index term: Radiographs, image quality

Radiology 143: 277, April 1982

DOCTOR Barnhard expresses concern over the lack of image quality standards and suggests that a diverse group be formed to develop a standardized method for evaluating image quality. His concerns are shared by most radiologists, however, it is our opinion that his comments do not accurately reflect the present state of knowledge concerning the physical parameters that define image quality or the ever-present human, chemical, and mechanical factors that degrade it.

Widely accepted standards for evaluation of image quality already exist. The descriptors of a screen-film system are its sensitometric curve, modulation transfer function (MTF), and level of radiographic mottle. With knowledge of these fundamental parameters, observer performance can be predicted by signal-to-noise ratio theory for simple phantom situations (*i.e.*, contrast-detail curves). Images of patients are infinitely more complex than those of phantoms; however, as is emphasized in the article by Gould *et al.* (1) which Dr. Barnhard mentions, radiologists will invariably rank images according to their signal-to-noise ratio for the task at hand. A lack of general understanding of this problem is well illustrated by Dr. Barnhard's own difficulties with the "fuzziness" of tomo-

grams made with a rare-earth screen-film combination. It has been noted in the literature that the quality of thin-section tomograms is particularly sensitive to radiographic mottle (2). The rare-earth screen-film combinations used in his department apparently have a great deal of mottle and are a poor choice for this particular examination. We strongly suspect that had Dr. Barnhard been aware of this he would have chosen a different combination.

The much more complex problem of image degradation by human, chemical, and mechanical factors is again one that committee-derived image quality standards could not solve but one that education and continuing concern can improve. Automatic processing as discussed by Dr. Barnhard is an excellent example. Several factors were responsible for the loss of image quality. The first emulsions employed in automatic processors were subject to noticeable wet pressure marks and other processing artifacts. These problems were even more pronounced in the first films used for 90-second processing, but were quickly corrected by film manufacturers. Other factors that were primarily educational in nature compounded these problems. The process was unforgiving in that it was no longer possible for darkroom personnel to sight-develop and compensate for improperly exposed films (3), and careful regular cleaning and maintenance were required for optimal results. Both of these problems still exist in many departments and require a continuing educational effort.

Dr. Barnhard states that no real standards exist and that changes come about based on varying criteria. Although not formally sanctioned, image quality standards do exist. For example, when a radiology department is considering changing to a new screen-film combination, their standard is usually the system they are currently using. Also, industry generally has standards. For a long time, Par Speed screens combined with a medium speed film was the standard of the screen-film industry. As digital radiographic units evolve, they will have to compete fa-

vorably with conventional radiographic systems in providing radiologists with patient information in order to gain widespread acceptance. That is, diagnostic information content is the primary criterion that determines change. Additional criteria are the convenience of technologists and radiologists as well as patient convenience and dose. Compared to the examinations of 1955 or even 1970, current studies generally provide comparable or superior diagnostic information at a fraction of the radiation dose.

In analyzing the examples that Dr. Barnhard gives, the importance of a sound understanding of the technical aspects of medical radiography is apparent. This understanding requires a solid grounding in the fundamentals during residency training followed by continuing educational efforts. However, the underlying concern that Dr. Barnhard has deals with how much (or how little) image quality is necessary for radiologists to perceive the clinically important information associated with various examinations. That is how much noise can be tolerated or how much can the MTF be degraded before the clinical efficacy of a study is sacrificed. Although a committee such as Dr. Barnhard envisions could focus attention on these questions, we believe the answers lie in scientific and educational efforts that demonstrate and communicate to radiologists the effects of changing various factors on routine clinical practice.

Gary T. Barnes, Ph.D.
Department of Diagnostic Radiology
The University of Alabama in Birmingham
Birmingham, AL 35294

References

1. Gould RG, Belanger B, Goldberg HI, Moss A. Objective performance measurements versus perceived image quality in intensified fluoroscopic or photospot images. *Radiology* 1980; 137:783-788.
2. Barnes GT, Witten DM. Film/screen considerations in tomography. *Radiology* 1974; 113:477-479.
3. Gustafson RB. Equipment design in relation to processors. In: Second image receptor conference: radiographic film processing. U.S. Department of Health, Education and Welfare Publication: (FDA) 77-8036, 1977, pp 77-79.

¹ From the Department of Diagnostic Radiology, The University of Alabama in Birmingham, Birmingham, AL. Received Sept. 30, 1981; accepted Dec. 14.

<あ と が き>

第13回画像分科会は、Barnes先生の講演を中心に「画像について語ろう」ということになりました。Barnes先生の業績のなかから、「Scatter」に関するものを2, 3抜き出してみました。参考にして下さい。

私どもが関心を高くするのは、「Image Quality : An Educational and Scientific Problem」（掲載論文の最後尾のもの）にみられますように、一つの高い知的関心を接続されていることです。

Barnes先生の学会での招待講演を含めて、この機会にアメリカの新進の放射線物理学者に接していただければ幸いです。 (山)

会費を納めて下さい。
1,000円です。
学会事務局宛でお願いします。

昭和58年4月1日発行
(社)日本放射線技術学会
画像分科会々長 内 田 勝
〒604 京都市中京区西ノ京壺井町88
二 条 プ ラ ザ 内
TEL (075)801-2238